CHAPTER 4

SYNTHESIS AND REACTIVITY OF METAL COMPLEXES SUPPORTED BY A PYRIDINE DIPHOSPHINE LIGAND WITH TUNABLE ELECTRONICS UTILIZING REMOTE LEWIS ACID BINDING

The text for this chapter was reproduced in part from:

Horak, K. T.; VanderVelde, D. G.; Agapie, T. *Organometallics*, **2015**, *34*, 4753-4765.

Abstract

Metal complexes supported by ligands with chemically modifiable pendant groups are of interest for controlling reactivity. We report on the coordination chemistry and reactivity of a multidentate phosphine ligand framework that contains Lewis acid binding sites. 3,5-Bis-(2-phosphinophenyl)-pyridine coordinates low oxidation state metal centers such as Ni^0 and Pd^0 via the phosphine donors and the π-system of the heterocycle. Electrophilic reagents such as $B(C_6F_5)_3$, Me^+, and BCy_2OTf were demonstrated to bind the available pyridine nitrogen, generating the Ni complexes (**2Ni-B(C$_6$F$_5$)$_3$**, **2Ni-Me**, **2Ni-BCy$_2$OTf**). Analogous compounds were prepared for Pd (**2Pd**, **2Pd-B(C$_6$F$_5$)$_3$**, **2Pd-H**). The effect of Lewis acid binding was evaluated by single crystal X-ray diffraction studies and spectroscopy. Lewis acid binding to **2Pd** leads to a stronger η^1 interaction between the metal and the heterocycle π-system. Ni binds in an η^2 fashion, but the Lewis acid-free species is not monomeric. Ni coordination results in disruption of pyridine aromaticity as indicated by localization of double- and single-bond character in the solid state. CO adducts were prepared for Lewis acid-free (**4Ni(CO)**) and Lewis acid–bound species (H^+–, Me^+–, and $B(C_6F_5)_3$–bound; **4Ni(CO)-H**, **4Ni(CO)-Me**, **4Ni(CO)-B(C$_6$F$_5$)$_3$**) that show a significant shift of the CO stretching frequency from 1930 cm^{-1} to 1966-1976 cm^{-1}, respectively, clearly indicating communication of ligand electronics to the metal center. A NO adduct (**5Ni**) with negligible metal-pyridine interactions was obtained upon sequential reaction of **2Ni** with $[OMe_3][BF_4]$ then $[NO][BF_4]$. Treatment of **2Ni** with silanes and boranes results in pyridine dearomatization involving heteroatom-H bond activation with the heteroatom binding to the pyridine nitrogen, and the hydrides delivered to the *ortho* positon of pyridine. This demonstrates that the electronics of the pendant

pyridine are drastically affected upon metal binding and enables unusual ligand-based substrate activation. The described chemistry highlights a strategy for tuning the properties of metal centers by ligand post-synthetic modifications.

INTRODUCTION

Alterations to ligand electronics can dramatically alter the properties of transition metal complexes. Efforts to develop chemically switchable ligands that show variable ligand electronics have been explored.[1] One such strategy has involved the binding of the Lewis acids to sites on the ligand framework to remotely tune the electronics.[2] This approach is amenable to the late-stage, modular tuning of ligand electronics, and serves as a way to rapidly assemble a range of complexes from a common precursor thereby avoiding the potentially time-consuming independent synthesis of multiple ligands. For SXS[3] and PXP[4] pincer ligands, where X is either an aryl or pyridine carbon or a pyridine or pyrazine nitrogen, remote hydroxyl, amino, or basic N-heterocycle sites have been incorporated into the ligand scaffold. However, the systematic functionalization of these groups with Lewis acids has not been reported, to the authors' knowledge. Our group has previously studied *meta*-substituted bis(phosphinoaryl)benzene ligand systems that bind in a P-arene-P pincer geometry (Figure 1).[5] Related diphosphines with other pendant π-systems have been reported.[6] *m*P_2Ni was found to coordinate a variety of ligands, and Ni methylidene and Ni imide complexes were implicated as intermediates that perform further intramolecular chemistry, such as CH amination. Complexes displaying Ni-ligand multiple bonding have been elegantly synthesized and studied by Hillhouse *et al.* and others.[7] As an alternative to the central arene donor in *m*P_2Ni, pyridine is known to bind a variety of electrophiles under mild conditions that can significantly alter the electronics and reaction chemistry of the heterocycle.[8] The properties of metal complexes bound to pyridine π-systems have been shown to be influenced by N-functionalization of the pyridine.[9] Herein, we report the synthesis and characterization of π-bound nickel and palladium complexes supported by a diphosphine ligand containing a π-coordinated pyridine

moiety that can be functionalized with electrophiles to alter the properties of the metal complex.

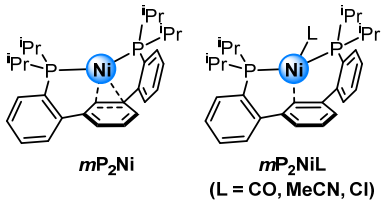

Figure 1. Ni complexes of *meta*-terphenyldiphosphine ligands.

RESULTS AND DISCUSSION

Section 4.1 Ligand Synthesis

Scheme 1. Synthesis of ligand 1

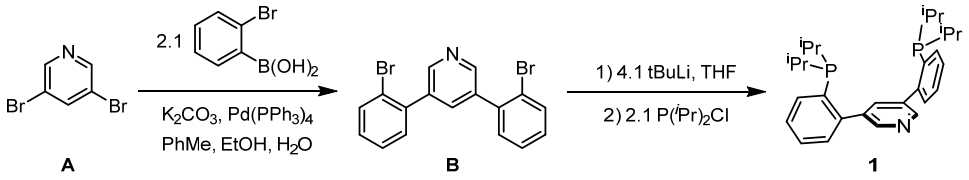

The desired ligand (**1**) was synthesized in two steps from commercially available starting materials. 3,5-(2-bromophenyl)pyridine (**B**) was synthesized from 3,5-dibromopyridine (**A**) and 2-bromophenylboronic acid in a palladium-catalyzed Suzuki coupling reaction and could be isolated as a colorless material following recrystallization. Subsequent phosphination was accomplished using a lithium halogen exchange reaction with *tert*-butyl lithium (*t*BuLi) followed by the addition of $P(^{i}Pr)_2Cl$ as an electrophile. Following workup, **1** could be isolated in gram quantities as a colorless powder.

Section 4.2 Synthesis and Electrophile Reactivity of Ni and Pd Complexes.

Metallations with nickel and palladium precursors were targeted as these metals are known to readily bind to related P-arene-P ligands (Scheme 2).[5a, 5b, 10] Mixing benzene solutions of **1**

and bis(1,5-cyclooctadiene)nickel(0) ($Ni(COD)_2$) in a stoichiometric ratio yielded **2Ni** as a brown solid after removal of volatile materials. The corresponding palladium complex (**2Pd**) was synthesized cleanly starting from palladium dimethyl (N,N,N',N'-tetramethylethylenediamine) (TMEDA) with mild heating to 70 °C for 16 hours. After workup **2Pd** could be isolated as an orange solid.

Scheme 2. Synthesis of nickel and palladium complexes

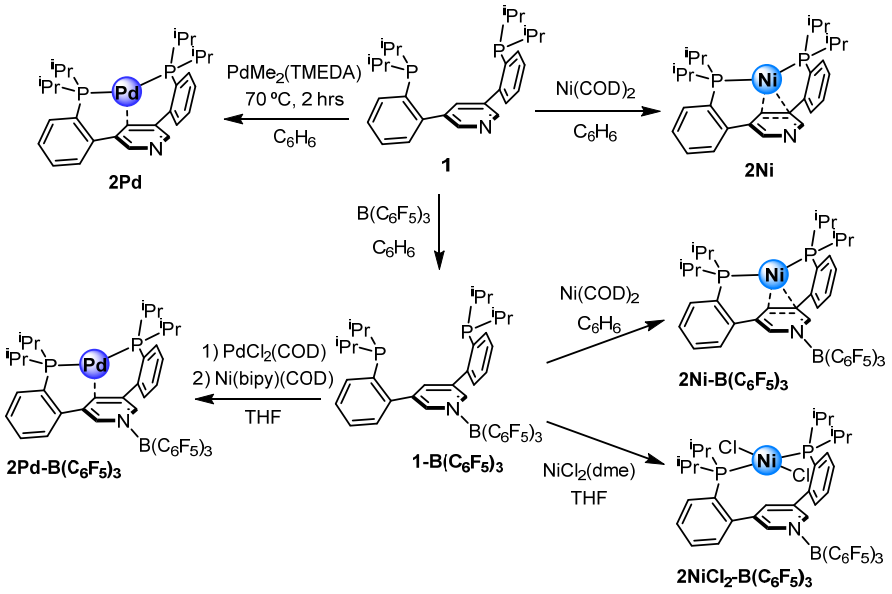

Solution NMR spectroscopic data for **2Ni** and **2Pd** are consistent with pseudo-C_s structures with single ^{31}P resonances at 40.32 and 33.76 ppm and two distinct isopropyl methine ^{1}H resonances at (2.28, 2.07) and (2.12, 1.86) ppm respectively. *m*P_2Ni has previously been shown to have a C_1 structure in the solid-state arising from η^2 coordination to the central arene π-system despite possessing pseudo-C_s solution NMR characteristics. This suggests that solution NMR data for **2Ni** and **2Pd** could arise from changes in metal-pyridine **π-system** coordination modes on the NMR time scale, resulting in apparent symmetry across the plane perpendicular to the pyridine ring containing the nitrogen and *para*-pyridyl carbon. The ^{31}P NMR spectrum at room temperature for **2Ni** is a broad singlet, which is suggestive of a slow

dynamic process. This is corroborated by the ^{1}H NMR where broadened resonances for the central pyridine protons are observed at 7.82 and 4.35 ppm for the *ortho*-pyridyl (C3 and C4 protons) and *para*-pyridyl (C1 proton) signals respectively. The proton signals are significantly upfield shifted from that of the free ligand at 8.96 and 7.89 ppm. This indicates significant disruption of pyridine electronic environment upon binding of the nickel center as seen with Ni complexes on related ligand platforms.[5a, 11] The *H*-C1 shows the largest upfield shift, consistent with that proton being directly bonded to the carbon atom that shows the strongest interactions with the nickel center. Cooling a sample of **2Ni** in d_8-toluene to -80 °C freezes out the fluxional process evident at room temperature leading to the observation of two pairs of coupling ^{31}P resonances at (46.07, 40.63 ppm ($^{2}J_{PP}$ = 75.0 Hz)) and (23.69, 22.79 ppm ($^{2}J_{PP}$ = 85.6 Hz)) of equal integration (Figure 2). These data suggest a dimerization process may be occurring likely arising due to pyridine coordination to a Ni center in another equivalent of complex. The pyridine protons of **2Pd** appear at 8.29 and 7.90 ppm for C3/C4 and C1 protons respectively. Interestingly, the *H*-C1 does not show any upfield shift and instead the *H*-C3/C4 show the larger upfield deviation from **1**. This is suggestive of comparatively weaker metal-pyridine π-system interaction and is consistent with palladium being less effective at backbonding than nickel.

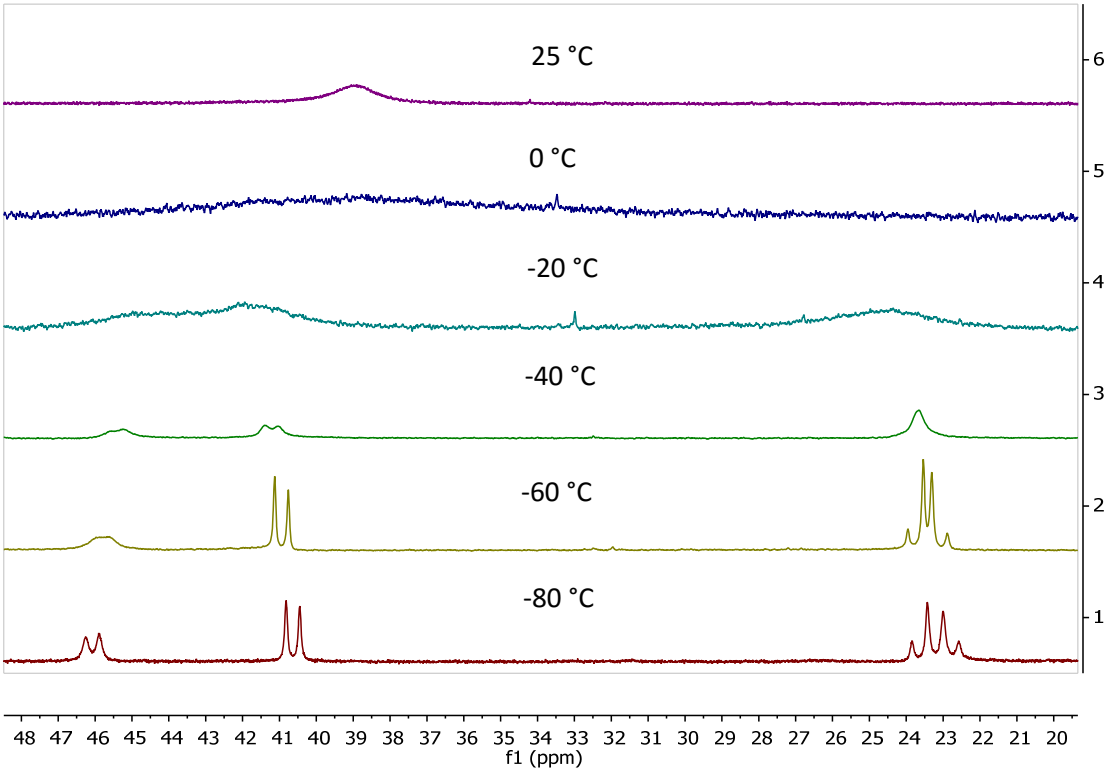

Figure 2. Variable temperature NMR (202 MHz ^{31}P, d_8-toluene) data for **2Ni**.

Attempts to selectively functionalize the pyridine nitrogen of **1** with Lewis acids prior to metallation were challenged by lack of selectivity relative to binding to phosphine. However, tris(pentafluorophenyl)borane ($B(C_6F_5)_3$) was found to coordinate to **1** exclusively through the pyridine nitrogen to yield **1-B(C_6F_5)$_3$** by NMR spectroscopy. **1-B(C_6F_5)$_3$** shows a single ^{31}P resonance at -5.58 ppm, which is close to that of the **1** (-5.75 ppm). The C3/C4 and C1 protons are also only slightly shifted and appear at 8.82 and 8.04 ppm respectively. ^{19}F NMR show three resonances at -131.46, -155.96, and -162.87 ppm shifted from the resonances of free borane (-130.29, -143.60, and -161.54 ppm), and consistent with four-coordinate boron.[12] These data are inconsistent with borane binding to a phosphine moiety as a significant ^{31}P shift is expected[13] in addition to asymmetry in the pyridine protons if only one equivalent of borane was bound. The observed binding selectivity is assigned to the large steric profile of

the borane, which disfavors binding to more sterically hindered phosphine donors compared to the pyridine nitrogen.

Scheme 3. Electrophile functionalization of pyridine nitrogen

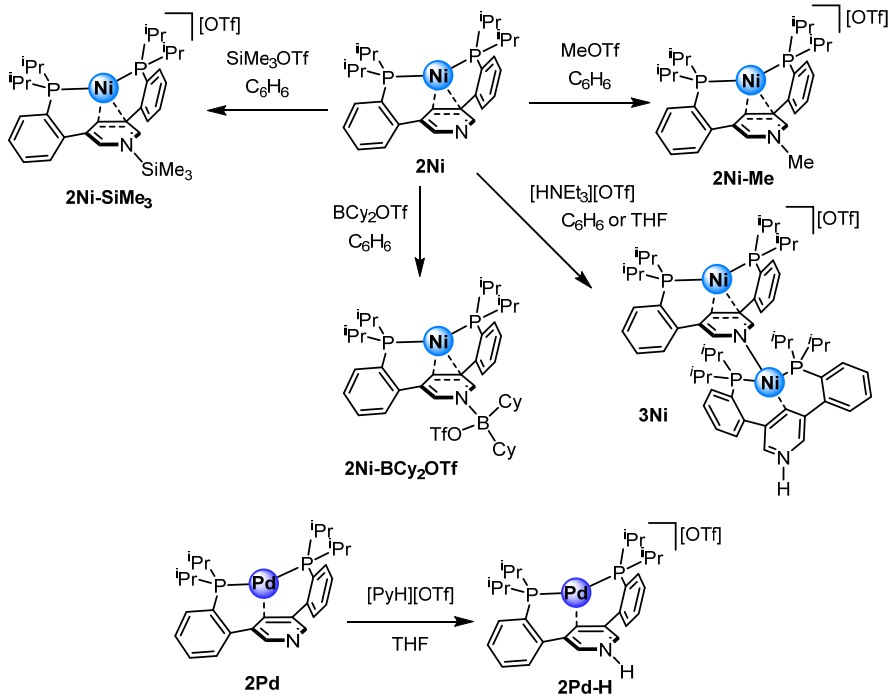

Analogous metallation procedures with $Ni(COD)_2$ were found to be effective with **1-B(C_6F_5)$_3$**, yielding **2Ni-B(C_6F_5)$_3$** as a dark brown solid in (Scheme 2). Additionally, a clean metallation with $NiCl_2$(dme) was observed to yield **2NiCl$_2$-B(C_6F_5)$_3$**. A one-pot procedure starting from Pd^{II} was found to be the most effective way to access **2Pd-B(C_6F_5)$_3$**. Initial metallation of $PdCl_2$(COD) produced a homogeneous orange solution, presumed to be a $PdCl_2$ complex supported by **1-B(C_6F_5)$_3$**. This was followed by reduction with (2,2'-bipyridine)(COD)nickel(0) to yield the desired Pd^0 complex. After workup **2Pd-B(C_6F_5)$_3$** was isolated as a bright pink solid.

^{1}H NMR data of **2Ni-B(C_6F_5)$_3$** and **2Pd-B(C_6F_5)$_3$** show single ^{31}P resonances at 41.94 and 34.06 ppm and two distinct isopropyl methine ^{1}H resonances at (2.07, 1.78) and (2.02,

1.69) ppm, respectively. These data are consistent with a pseudo-C_s symmetric structure or a fluxional process in solution. Interesting only small differences in ^{31}P NMR shifts are seen between **2Ni** and **2Ni-B(C_6F_5)$_3$** despite the binding of B(C_6F_5)$_3$ to the pyridine nitrogen, indicating that ^{31}P NMR is either not a good indicator of electronic changes caused by Lewis acid binding or that the P-atoms are not significantly affected. ^{19}F NMR data show sets of three signals (**2Ni-B(C_6F_5)$_3$**: -131.35, -157.46, -163.85 ppm; **2Pd-B(C_6F_5)$_3$** -131.04, -157.36, -163.73 ppm), at similar chemical shifts as for **1-B(C_6F_5)$_3$**, consistent with pyridine coordination of B(C_6F_5)$_3$. In contrast to ^{31}P NMR, the ^{1}H NMR spectra of compound **2Ni-B(C_6F_5)$_3$** show a further upfield shift of the pyridine protons, with the *H*-C1 signal showing at 3.18 ppm compared to 4.35 ppm for **2Ni**. This shift is likely due to the electronic effect caused by binding of the Lewis acid. The electron withdrawing B(C_6F_5)$_3$ group to the pyridine nitrogen results in the central pyridine ring becoming a better π-acceptor ligand for the electron-rich Ni^0 center. Consequently, strong metal-pyridine π-system interactions result in an even greater upfield shift of the *H*-C1 compared to **2Ni**. Consistent with the NMR data for analogous nickel complex, **2Pd-B(C_6F_5)$_3$** also shows a significant upfield shift in the central pyridine protons with the *H*-C3/C4 signals at 7.69 and *H*-C1 signal at 6.39 ppm. While **2Pd** showed a *H*-C1 pyridine resonance essentially the same as free phosphine, **1**, the upfield shift in **2Pd-B(C_6F_5)$_3$** indicates a significant metal-pyridine π-system interaction that results from the more electron deficient borane-bound pyridine.

2NiCl$_2$-B(C_6F_5)$_3$ is not expected to have a metal-pyridine π-system interaction based on previous reports from group for a related ***m*P$_2$NiCl$_2$** compound.[5a] Consistent with this assignment is the absence of upfield shifted NMR resonances corresponding to the central pyridine ring. Instead a substantial downfield shift of the central pyridine C1-*H* resonance compared to free ligand is observed (δ(ppm) **2NiCl$_2$-B(C_6F_5)$_3$**: 10.84, **1-B(C_6F_5)$_3$**: 8.04). A

comparable shift in the C3/C4 proton resonances is not observed again highlighting to increased sensitivity of the C1 protons to the metal center (δ(ppm) **2NiCl$_2$-B(C$_6$F$_5$)$_3$**: 8.57, **1-B(C$_6$F$_5$)$_3$**: 8.82). **2NiCl$_2$-B(C$_6$F$_5$)$_3$** shows two distinct methine proton resonances (2.46, 1.56 ppm) and a single ^{31}P signal at 7.51 ppm. These data are consistent with a pseudo-C_s symmetric structure or a fluxional process in solution. This unusual chemical shift for the C1 proton (10.42 ppm) has been previously observed in a related complex, ***m*P$_2$NiCl$_2$**, again supporting a similar structural assignment.

To expand the series of Lewis acids investigated, functionalization of the pyridine nitrogen was attempted starting with metallated species, **2Ni** and **2Pd**, by reaction with various electrophiles. **2Ni** was found to react quantitatively with methyl triflate and dicyclohexylboron triflate to yield **2Ni-Me** and **2Ni-BCy$_2$OTf,** respectively (Scheme 3), that were both obtained as dark brown solids. Trimethylsilyl triflate was also found to generate a new green species, **2Ni-SiMe$_3$**, by NMR. However, this compound was not stable likely due to loss of silylation of the glass, though the use of presilylated NMR tubes improved the lifetime of the compound. NMR evidence indicates selective derivatization of the pyridine nitrogen by the electrophile rather than a nickel-based reaction such as an oxidative addition. **2Ni-Me** displays a single ^{31}P resonance at 31.13 ppm and two distinct isopropyl methine ^{1}H resonances at 2.57 and 2.45 ppm, consistent with a C_s symmetric structure or a fluxional process in solution. The methyl protons that do not correspond to the isopropyl substituents of **2Ni-Me** appear at 2.77 ppm and do not show ^{31}P coupling. This chemical shift and lack of 3-bond coupling to phosphorus indicate that methylation has not occurred at the metal center, but rather at the pyridine nitrogen. Of particular note is the chemical shift for the *H*-C1 of the pyridine which appears as a triplet (J =5.03 Hz) at 1.95 ppm, *further* upfield than the aliphatic isopropyl methine protons. ^{31}P decoupling the ^{1}H spectrum results in an singlet resonance for the *H*-C1,

indicating that coupling to two equivalent ^{31}P nuclei results in the observed triplet. This significantly upfield shifted *H*-C1 and *H*-C3/C4 (6.76 ppm) resonances again indicates a substantial Ni-pyridine π-system interaction that is stronger than either **2Ni** or **2Ni-B(C_6F_5)$_3$**. This likely arises from the cationic nature of the electrophile bound to the pyridine nitrogen ($B(C_6F_5)_3$ vs Me^+) which results in a substantially more electron deficient central pyridine. For **2Ni-BCy$_2$OTf** the cyclohexyl substituents complicate the aliphatic region of the ^1H NMR spectrum. However, the *H*-C1 can be assigned to a peak at 3.45 ppm, close to that of **2Ni-B(C_6F_5)$_3$**. The ^{31}P NMR chemical shift 42.29 ppm again is only slightly shifted from **2Ni**.

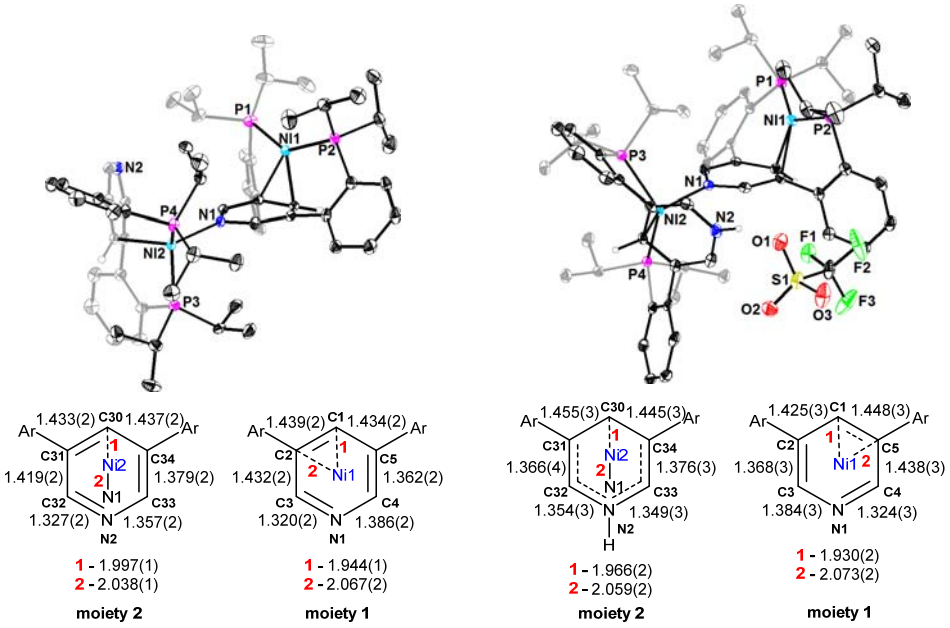

Figure 3. Solid-state structures and selected bond metrics for (left to right) **2Ni** and **3Ni**. Hydrogen atoms and solvent have been omitted for clarity.

The reaction of triethylammonium triflate (Scheme 3) with **2Ni** selectively forms a dinuclear mono-protonated species, **3Ni**, (Figure 1), which precipitates out of reaction mixtures when run in benzene though tetrahydrofuran is also compatible as a solvent (vide infra). Pyridinium triflate was found to cleanly react with **2Pd** to produce a mononuclear

complex, as a pink material (**2Pd-H**). Reactions of **2Pd** with other electrophiles yielded complex mixtures of products and were not pursued further. In line with other complexes, **2Pd-H** is C_s symmetric in solution with a ^{31}P NMR resonance at 32.08 ppm and two distinct isopropyl methine ^{1}H resonances at 2.77 and 2.30 ppm in d_3-acetonitrile. Upfield shifted *H*-C3/C4 (7.28 ppm) and *H*-C1 (6.16 ppm) resonances are observed, and are consistent with metal-pyridine π-system interactions that are stronger than in **2Pd** and comparable to those seen in **2Pd-B(C$_6$F$_5$)$_3$**. Importantly, the proton resonance derived from the pyridinium triflate is seen as a broad resonance at 9.88 ppm. This is a region is consistent with a pyridinium moiety not a palladium hydride. Furthermore, no apparent coupling to ^{31}P nuclei is observed, which would be expected in the case of a Pd-H moiety. These results agree with the results of reactivity **2Ni** with electrophiles, which demonstrate that selective derivatization of the pyridine nitrogen is also possible with Pd.

Solid-state structures were obtained by single crystal X-ray diffraction (XRD) studies. **2Ni** was found to crystallize as a dinuclear species with the pyridine nitrogen of one equivalent of complex (moiety 1) binding to the nickel center of the other (moiety 2) (Figure 3). The observed dimerization in the solid state agrees well with the ^{31}P solution NMR data obtained for **2Ni** at -80 °C suggesting the reversible pyridine coordination is responsible for the observed broadening of ^{1}H and ^{31}P signals at room temperature. Consistent with structures of Ni^0 complexes on related ligands,[5a, 5c, 11] the metal center in moiety 1 of **2Ni** binds to the central pyridine in an η^2 fashion with Ni–C1 and Ni–C2 distances of 1.944(1) and 2.067(1) Å respectively. Disrupted aromaticity is evident from the central pyridine bond metrics by comparing bond distances for C2–C3 (1.432(2) Å) to C4–C5 (1.362(2) Å) and C3–N1 (1.320(2) Å) to C4–N1 (1.386(2) Å). The significant differences seen in each of these pairs of bond distances highlights the partial localization of double bond character around the central

pyridine ring. Significant backbonding from Ni is also evident from the C1–C2 distance (1.439(2) Å), which is longer than all other C–C bond in the pyridine.

Moiety 2 of **2Ni** shows η^1 coordination of nickel to the central pyridine, a binding mode shift observed upon acetonitrile coordination in a related Ni^0 complex supported by a *meta*-substituted bis(phosphinoaryl)benzene ligand (Figure 1).[5a] This binding mode change results in a longer Ni–C30 contact of 1.997(1) Å. Aromaticity still appears to be disrupted within the pyridine ring, though to a lesser extent than seen in moiety 1 since the compared distances (C31–C32: 1.419(2) C33–C34: 1.379(2)) and (C32–N2: 1.327(2) C33–N2: 1.357(2)) show smaller differences. This portion of the structure of **2Ni** demonstrates the potential for flexible metal-pyridine π-system interactions that varies with ligand coordination.

Structurally characterized complexes of Ni and Pd with a π-bound pyridine are very rare. The only example to the authors' knowledge is a bis-N-heterocyclic carbene complex of Ni bound η^2 to the C3-C4 positions of a pyridine coordinated via the nitrogen to $AlMe_3$.[14] Though an analogous coordination mode is observed in moiety 1 of **2Ni**, the average Ni–C distances are longer by 0.025 Å in **2Ni**. This is consistent with weaker backbonding into the coordinated C_2 fragment as evidenced from the 0.17 Å shorter C–C distance in **2Ni**. Disrupted aromaticity is also evident in the literature compound though differences in C–C and C–N distances range between 0.01-0.035 Å. This is likely attributable to electronic differences attributable to the N-heterocyclic carbene ligands as well as the coordination of $AlMe_3$ rather than the Ni center of moiety 2.

The solid-state structure of **3Ni** is reminiscent of that of **2Ni**, again with a 3-coordinate nickel complex (moiety 1) binding through its pyridine nitrogen to a protonated equivalent of complex (moiety 2). The bond metrics for moiety 1 of **3Ni** are similar to the analogous ones

of **2Ni**, indicative only of minor perturbation as the site of protonation is quite remote. More substantial changes are seen in bond metrics of moiety 2 of **3Ni**. A different pattern of disruption of aromaticity is observed with similar C31–C32/C33–C34 (1.366(4), 1.376(3) Å) and C32–N2/C33–N2 (1.354(3), 1.349(3) Å) bond distances seen on opposite sides of the pyridine ring relative to the N2-C30 vector. Consistently, C30–C31 and C30–C34 distances are both lengthened, at 1.455(3) and 1.445(3) Å, respectively. Contraction of the Ni–C30 distance to 1.930(2) Å suggests a stronger interaction between the metal and the π-system compared to **2Ni**. These distances are consistent with partial isolation of C30 from the π-system of the pyridine, which results in delocalization across the remaining 5-atoms. The above structural parameters demonstrate the plasticity of pyridine π-system and its potential to rearrange as a function of Lewis acid functionalization of the pyridine nitrogen.

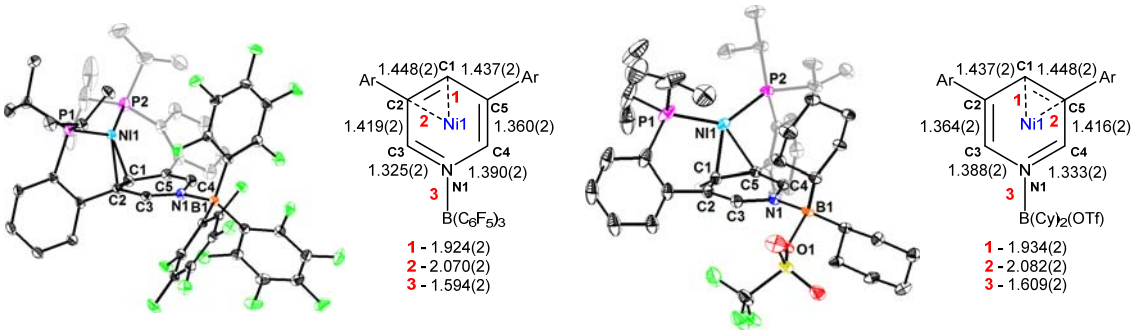

Figure 4. Solid-state structures and selected bond metrics for **2Ni-B(C_6F_5)$_3$** and **2Ni-BCy$_2$OTf**. Hydrogen atoms have been omitted for clarity.

2Ni-B(C_6F_5)$_3$ and **2Ni-BCy$_2$OTf** both crystallize as discrete complexes (Figure 4). They display four-coordinate boron centers. The nickel center is coordinated in an η^2 fashion to the central pyridine in a manner comparable to moiety 1 of **2Ni** and **3Ni**. Furthermore, the distortions of observed in the pyridine moiety are very similar between **2Ni-B(C_6F_5)$_3$, 2Ni-BCy$_2$OTf** and moiety 1 of **2Ni** and **3Ni**. Overall, the structural parameters of these complexes are indicative of stronger interactions between the metal center and the π-bound

heterocycle compared to moiety 2 of **2Ni** where the pyridine nitrogen is not coordinated. However, this comparison must be taken cautiously given that the metal center in moiety 2 of **2Ni** is four-coordinate, while the other compounds display three-coordinate metal centers. In the case of **2Ni**, the comparison is complicated by the dinuclear nature of the crystallized complex. In contrast, Pd complexes and carbon monoxide adducts of Ni complexes (vide infra) provide better points of reference as they are mononuclear in both Lewis acid-bound and –free states.

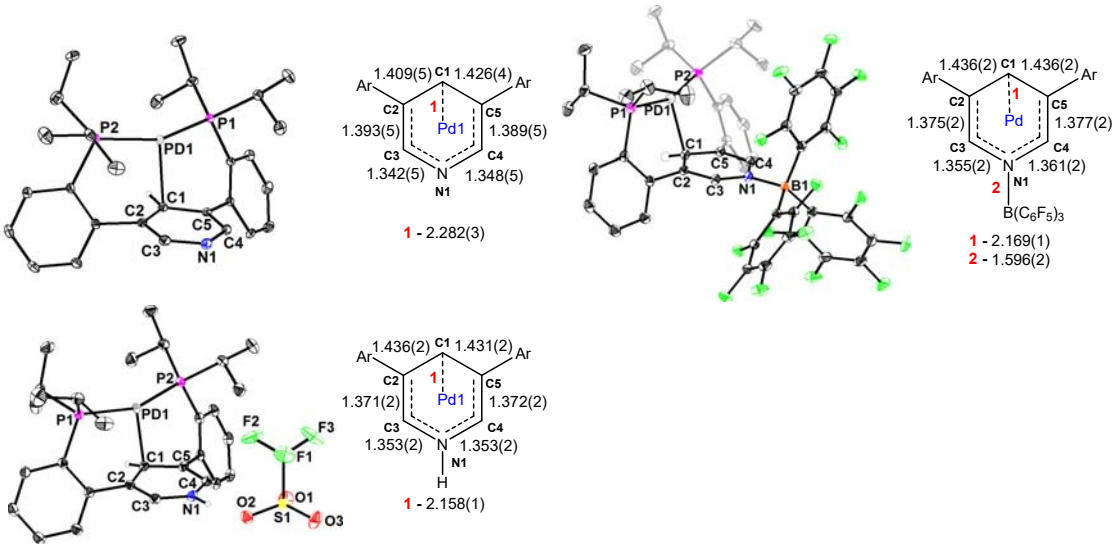

Figure 5. Solid-state structures and selected bond metrics for **2Pd**, **2Pd-B(C_6F_5)$_3$**, and **2Pd-H**. Hydrogen atoms have been omitted for clarity.

As mentioned above, **2Pd**, **2Pd-B(C_6F_5)$_3$**, and **2Pd-H** crystallize as the discrete monomers allowing the direct comparison of the effect of the electrophile on the structural parameters (Figure 5). All complexes show η^1 coordination to the central pyridine ring with Pd–C1 distances of 2.282(3), 2.169(1), and 2.158(1) Å respectively. The significant shortening of the Pd–C1 distance is attributed at a stronger interaction between the electron rich Pd^0 and the more electron deficient borane and proton functionalized pyridine moieties. Symmetric distortions of central pyridine bond metrics relative to the N1-C1 vector are seen, with C2–

C3 and C4–C5 (0.002 Å average change) as well as C3–N1 and C4–N1 (0.004 Å average change) showing negligible differences. However, between complexes differences can be observed. An elongation of C1–C2 and C1–C5 bonds is seen in **2Pd-B(C_6F_5)$_3$** and **2Pd-H** (ranging between 1.436(2) to 1.431(2) Å) vs **2Pd** (1.409(5) and 1.426(4) respectively) again suggestive of a stronger metal-pyridine interaction. C2–C3 and C4–C5 distances shorten by an average of 0.015 and 0.038 Å while C3–N1 and C4–N1 elongate by an average of 0.013 and 0.008 Å for **2Pd-B(C_6F_5)$_3$** and **2Pd-H** respectively relative to **2Pd**. The geometry around palladium is T-shaped with a P1–Pd1–P2 angle of 155.65(3), 160.89(2), 156.97(1) ° for **2Pd**, **2Pd-B(C_6F_5)$_3$**, and **2Pd-H** respectively. For comparison, the P1–Ni–P2 angles are between 133 and 139 in compounds **2Ni-B(C_6F_5)$_3$** and **2Ni-BCy$_2$OTf**, moiety 1 of **2Ni** and **3Ni**. Due to the metal center's increased size, the coordination angle of the diphosphine is larger with palladium. Additionally, the coordination flexibility of the palladium complexes may be limited and a binding akin to that of molecule 1 of **2Ni** may not be sterically accessible.

Section 4.3 Binding of Small Molecules to Ni Complexes

To further study the effect of pyridine modification of ligand electronics on the properties of the metal centers, a series of carbon monoxide adducts was pursued to take advantage of CO as a spectroscopic reporter based on its infrared stretching frequency (Scheme 4). Treatment of with one equivalent of CO was found to quantitatively convert **2Ni**, **2Ni-B(C_6F_5)$_3$**, and **2Ni-Me** to the corresponding mono-CO adducts, **4Ni(CO)**, **4Ni(CO)-B(C_6F_5)$_3$**, and **4Ni(CO)-Me** respectively. The ν_{CO} for **4Ni(CO)** appears 1930 cm^{-1}. The related complex supported by the *meta*-terphenyl diphosphine ligand shows a more activated CO (ν_{CO} = 1916 cm^{-1}) indicative of the more electron rich benzene vs pyridine resulting in a metal center more prone to undergo π-backbonding with CO.[5a] The binding of Lewis acids to

the pyridine nitrogen results in a shift to higher ν_{CO} values as the pyridine ring becomes more electron deficient and competes as an acceptor ligand with the CO (ν_{CO} (cm^{-1}): **4Ni(CO)-B(C_6F_5)$_3$** (1976) and **4Ni(CO)-Me** (1966)). The addition of an equivalent of pyridinium triflate to **4Ni(CO)** results in the quantitative formation of **4Ni(CO)-H** which shows a ν_{CO} of 1975 cm^{-1}. Interestingly, **4Ni(CO)-B(C_6F_5)$_3$** and **4Ni(CO)-H** show similar ν_{CO} frequencies despite the difference in charge. It is notable that changing the supporting π-system from benzene to pyridine has a smaller effect (~14 cm^{-1}) on ν_{CO} compared to binding Lewis acids to the pyridine nitrogen (36 to 45 cm^{-1}).

Scheme 4. Synthesis of small molecule-coordinated Ni complexes

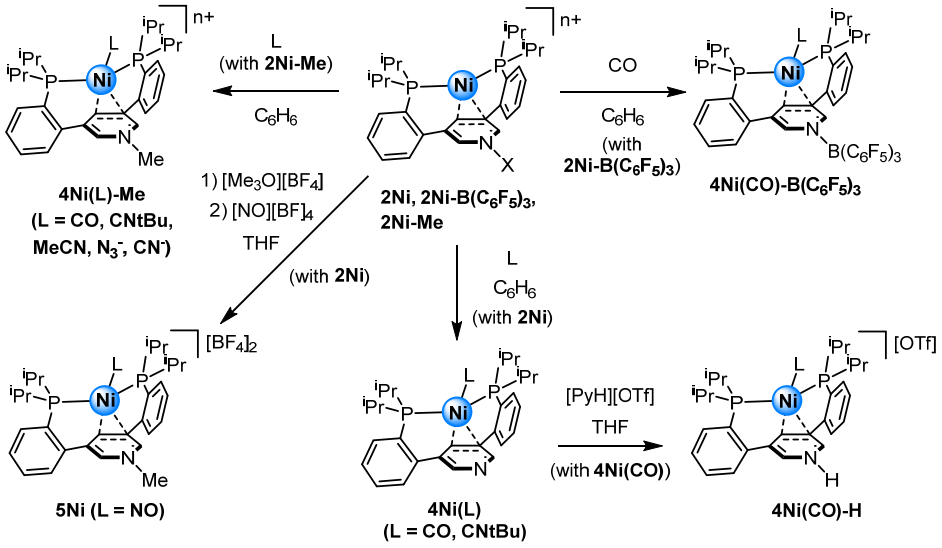

NMR data indicate that the introduction of the CO ligand significantly alters the metal-pyridine interaction (Figure 6). Each complex shows NMR data that is consistent with a C_s symmetric species or a fluxional process in solution as seen from the sharp ^{31}P singlet (δ(ppm): **4Ni(CO)** (33.83), **4Ni(CO)-B(C_6F_5)$_3$** (31.84), **4Ni(CO)-Me** (34.74), and **4Ni(CO)-H** (35.69 in CD_3CN**)**) and two distinct ^1H signals observed for the isopropyl methines (δ(ppm): **4Ni(CO)** (2.33, 2.06), **4Ni(CO)-B(C_6F_5)$_3$** (2.17, 1.74), **4Ni(CO)-Me** (2.27, 1.98), and

4Ni(CO)-H (2.82, 2,49 in CD_3CN)). The signal for the *H*-C1 ((δ(ppm): **4Ni(CO)** (6.23), **4Ni(CO)-B(C_6F_5)$_3$** (4.61), **4Ni(CO)-Me** (4.53), and **4Ni(CO)-H** (4.80 in CD_3CN)) and C3/C4 ((δ(ppm): **4Ni(CO)** (6.23), **4Ni(CO)-B(C_6F_5)$_3$** (4.61), **4Ni(CO)-Me** (4.53), and **4Ni(CO)-H** (4.80 in CD_3CN)) shifts downfield indicating a weaker metal–pyridine interaction, a consequence of competing π-backbonding between metal and pyridine vs CO. Corroborating the similarities in the IR data, both **4Ni(CO)-B(C_6F_5)$_3$** and **4Ni(CO)-Me** show similar chemical shifts for the *H*-C1 despite the charge difference.

Solid-state structures for **4Ni(CO)** and **4Ni(CO)-H** were obtained allowing for comparison to the CO-free analogs and evaluation of the effect of pyridine derivatization with monometallic Ni species (Figure 7). Both **4Ni(CO)** and **4Ni(CO)-H** show η^2 coordination to the central pyridine moiety, differing from **mP$_2$Ni-CO** which shows η^1 coordination.[5a] The shortest Ni–C_{ring} distance is 2.254(1) Å in **mP$_2$Ni-CO** which is longer than in both **4Ni(CO)** (2.119(1) Å) and **4Ni(CO)-H** (2.029(1) Å) consistent with stronger interactions between the electron rich Ni^0 center and the electron deficient heterocycle relative to benzene. These differences in the interactions with the π-systems are corroborated by the ν_{CO} values. Disrupted aromaticity is observed in both **4Ni(CO)** and **4Ni(CO)-H** with significant differences in bond metrics observed for C2–C3 vs C4–C5 as well as C3–N1 vs C4–N1 indicating partial localization of double and single bonds. The shortest Ni-pyridine interactions for **4Ni(CO)** and **4Ni(CO)-H**, 2.119(1) and 2.029(1) Å respectively, are elongated relative to moiety 2 of **2Ni** (1.997(1) Å) and **3Ni** (1.966(2) Å), respectively, consistent with the CO ligand being overall more acidic than the N-bound pyridine and leaving the metal center less prone to backbonding to the π-system of pyridine. It is worth noting that the pattern of aromaticity disruption (localized double bond character) and coordination mode are different between **4Ni(CO)** and **4Ni(CO)-H** vs moiety 2 of **2Ni** and **3Ni** despite

both complexes being 4-coordinate at nickel. This structural difference may be a consequence of CO being smaller than substituted pyridine and accommodating η^2-coordination to the central π-system.

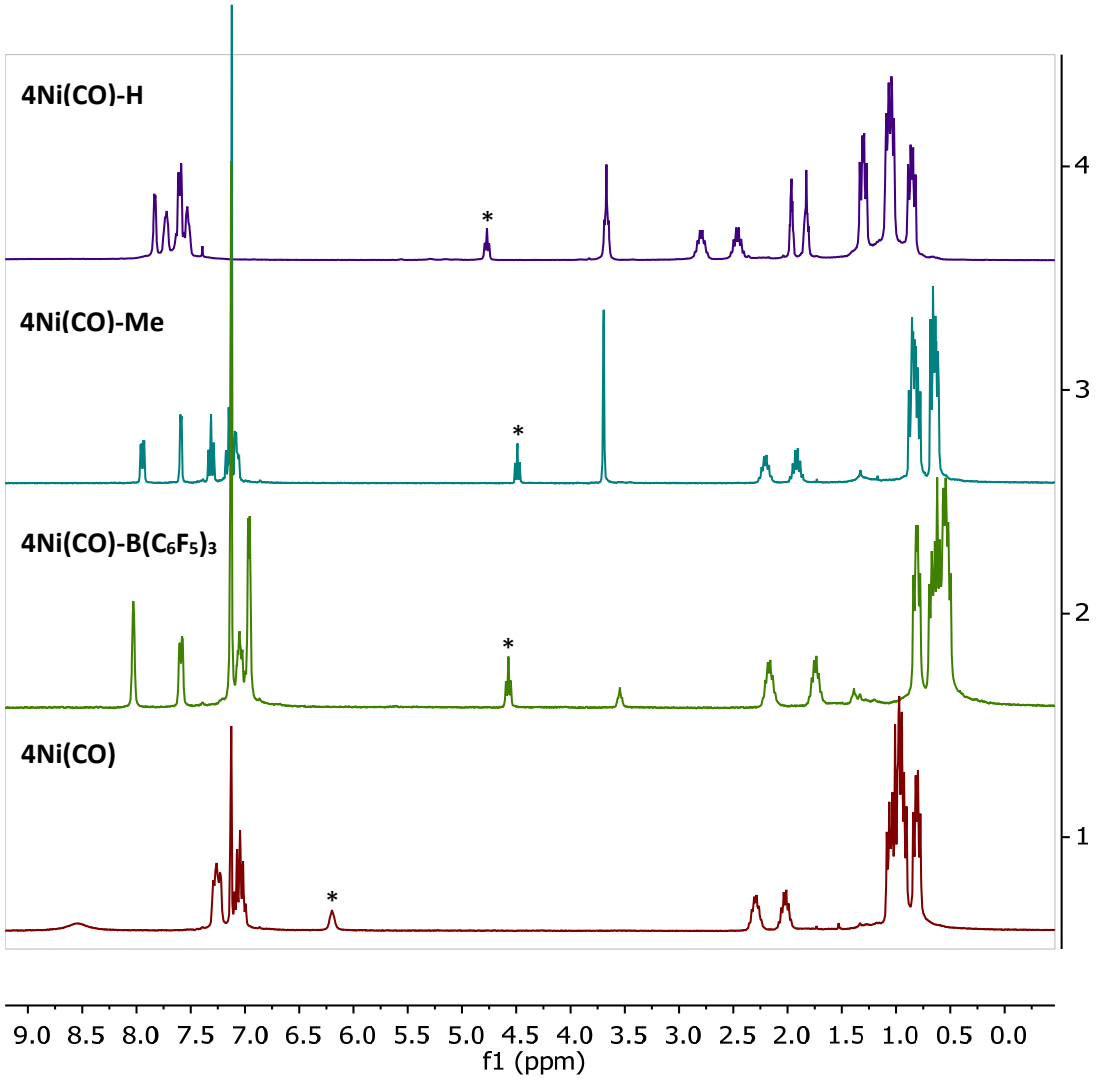

Figure 6. ^{1}H NMR comparison for all isolated Ni monocarbonyl complexes. Peaks denoted by an asterisk indicate the C1 proton of the central pyridine ring. All spectra are taken in C_6D_6 with the exception of **4Ni(CO)-H** which was obtained in CD_3CN.

Comparison between **4Ni(CO)-H** and **4Ni(CO)** provides insight into the effect of protonation on pyridine coordination to metal. **4Ni(CO)-H** shows shorter Ni-C contacts vs **4Ni(CO)** consistent with stronger interaction between the metal and pyridine in **4Ni(CO)-**

H. Additionally, the C1–C5 distance of the Ni-coordinated C_2 moiety is shorter in **4Ni(CO)** (1.416(2) Å) compared to **4Ni(CO)-H** (1.441(2) Å), suggesting weaker backbonding into the pyridine in **4Ni(CO)**. These effects are likely due to the more electron deficient pyridinium moiety being a better π-acceptor from the electron rich Ni^0 center compared to pyridine.

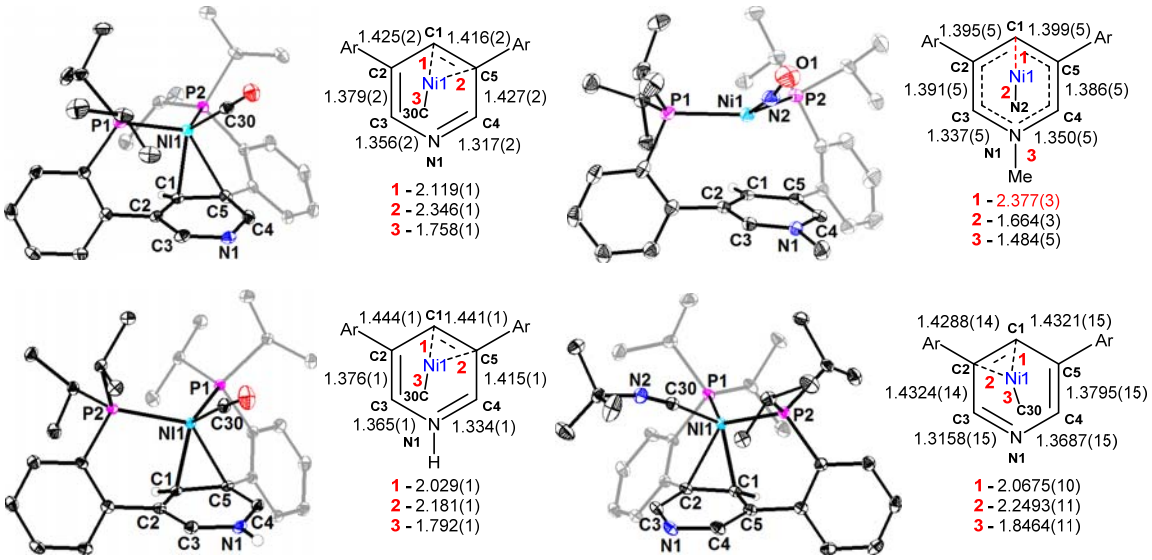

Figure 7. Solid-state structures and selected bond distances of **4Ni(CO)**, **4Ni(CO)-H**, **5Ni**, and **4Ni(CN*t*Bu)**. Hydrogen atoms and solvent have been omitted for clarity.

To test the ability of ligands derivatized at pyridine to support coordination of other donors to Ni, reaction with nitrosonium ion was pursued as an isoelectronic analog of carbon monoxide. **2Ni** reacts with trimethyloxonium tetrafluoroborate ($[OMe_3][BF_4]$) in THF to *in situ* generate the N-methylated complex. Subsequently, $[NO][BF_4]$ was added causing color change from a dark brown to a blue-brown solution. Following work up, the desired complex, **5Ni**, was isolated as a dark blue crystalline solid. NMR spectra recorded in d_3-acetonitrile indicated the formation of a species that showed a broad ^{31}P signal at 31.31 ppm. The chemical shift of the C1 (7.55 ppm) and C3/C4 protons (9.01 ppm) appear in the aromatic region suggesting weaker metal-pyridine π-system interactions than any of the CO complexes. This is corroborated by the solid-state structure. The structure of **5Ni** shows substantial differences

from all other nickel complexes synthesized. A negligible Ni-pyridine interaction is present as seen from the long Ni–C1 distance of 2.377(3) Å. The sum of the P–Ni–P and P–Ni–N angles is equal to 350.78 ° and is approaching the theoretical value for ideal trigonal planar coordination. Therefore, this complex represents a rare example of a structurally characterized three-coordinate Ni-NO complex where both other donors are phosphines.[15] Central pyridine distances also indicate a negligible Ni-heterocycle interaction as C–C (1.386(5) to 1.399(5) Å) and C–N distances, 1.337(5) and 1.350(5) Å for C3–N1 and C4–N1 respectively, are quite similar. The NO stretching frequency for **5Ni** appears at 1846 cm^{-1} (IR). The Ni–N2–O1 angle is 163.1(4) ° which is consistent with literature linear nitrosyl moieties bound to Ni.[16] These data indicate that the pyridinium ring cannot compete with the nitrosonium ligand for coordination of nickel.

Following the initial success with nitrosonium coordination, the binding of other small molecules was pursued. **2Ni** was found to readily bind *tert*-butyl isocyanide to produce **4Ni(CN*t*Bu)** although the partial formation of free ligand was also observed (Scheme 4). Analogous reactions with **2Ni-B(C_6F_5)$_3$** resulted in a complicated mixture of products, likely resulting from the steric profile of the B(C_6F_5)$_3$ moiety. **2Ni-Me** was found to readily coordinate *tert*-butyl isocyanide to yield **4Ni(CN*t*Bu)-Me**. The addition of other small molecules such as cyanide, azide, and acetonitrile to **2Ni-Me** results in quantitative binding to the Ni-center to produce **4Ni(CN)-Me**, **4Ni(N_3)-Me**, and **4Ni(MeCN)-Me** respectively. Including **5Ni**, N-methylated Ni complexes coordinate a variety of small molecules of charge varying from anionic (CN^- and N_3^-), to neutral (MeCN, CN*t*Bu, and CO), and even cationic in the case of nitrosonium.

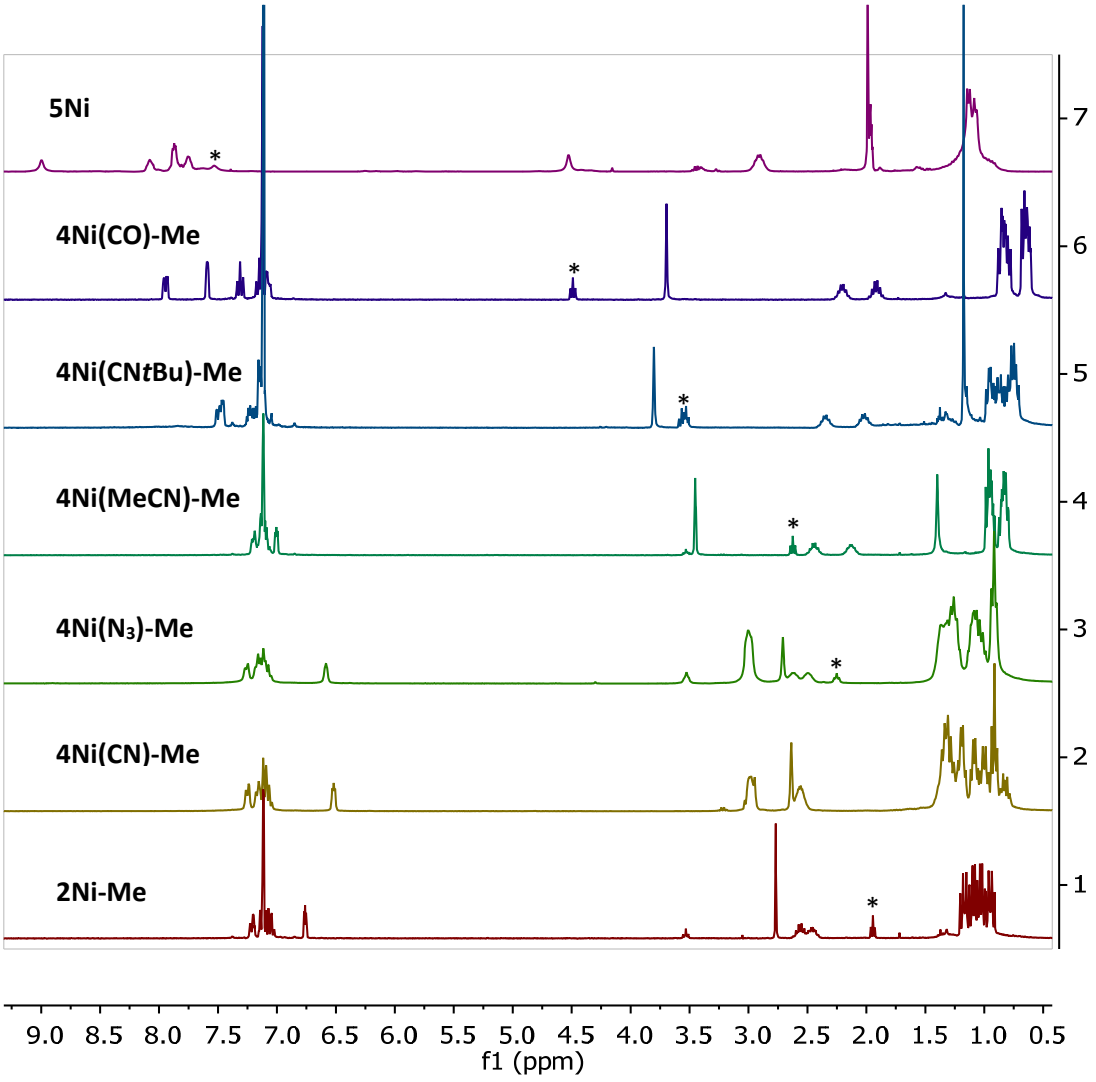

Figure 8. ^{1}H NMR comparison for all isolated N-methylated Ni complexes. Peaks denoted by an asterisk indicate the C1 proton of the central pyridine ring. All spectra are taken in C_6D_6 with the exception of **5Ni** which was obtained in CD_3CN.

As carbon monoxide is expected to be a better π-acid than *tert*-butyl isocyanide, **4Ni(CO)** is expected to display a weaker Ni-pyridine π-system interaction compared to **4Ni(CN*t*Bu)** as the coordinated ligand competes better for electron density with the heterocycle. This is borne out in the comparison of solution NMR data for **4Ni(CO)** and **4Ni(CN*t*Bu)**. Both complexes show substantially upfield shifted resonances for the central pyridine protons (**4Ni(CN*t*Bu)** δ(ppm) *H*-C1: 5.51, *H*-C3/C4 8.17; **4Ni(CO)** δ(ppm) *H*-C1: 6.23, *H*-C3/C4

8.58) consistent with a strong Ni-pyridine π-system interaction. However, for both *H*-C1 and *H*-C3/C4 resonances for **4Ni(CNtBu)** appear further downfield compared to **4Ni(CO)** (Δδ(ppm) *H*-C1: 0.72, *H*-C3/C4: 0.41) indicating more backbonding from the Ni center into the pyridine ring for **4Ni(CNtBu)**. Both complexes show a comparable pair of ^{1}H resonances (δ(ppm): **4Ni(CO)** (2.35, 2.06), **4Ni(CN*t*Bu)** (2.41, 2.11)) corresponding to the methine protons. Single resonances are observed by ^{31}P NMR (δ(ppm): **4Ni(CO)** 33.83, **4Ni(CN*t*Bu)** 36.56). Overall the effect of a change in π-acidity of the donor ligand moves the C1-H chemical shift by roughly half that resulting from the binding of $B(C_6F_5)_3$ to the pyridine nitrogen (*H*-C1 δ(ppm): **4Ni(CO)-B(C_6F_5)$_3$** 4.61). Crystals suitable for XRD experiments were obtained for **4Ni(CN*t*Bu)** allowing for comparisons in the solid-state with **4Ni(CO)** (Figure 7). Both complexes show η^2 coordination modes with a shorter average Ni–C distance (**4Ni(CO)** 2.23 Å, **4Ni(CN*t*Bu)** 2.16 Å) seen for **4Ni(CN*t*Bu)** consistent with a stronger Ni-pyridine π-system interaction. Otherwise, central pyridine bond lengths are consistent localized double bond character due to Ni coordination.

In a similar way, NMR comparisons across the series of **4Ni(L)-Me** (L = CN^-, N_3^-, MeCN, CN*t*Bu, CO) and **5Ni** allows for an assessment the strength of the Ni-pyridine π-system interaction with a wide variety of small molecules while holding the pyridine substitution constant (Figure 8). A clear trend in the chemical shift of the C1-*H* proton can be seen with the more π-acidic donors resulting in a more downfield resonance (C1-*H* δ(ppm): **5Ni** 7.55 (CD_3CN), **4Ni(CO)-Me** 4.49, **4Ni(CN*t*Bu)-Me** 3.57, **4Ni(MeCN)-Me** 2.62, **4Ni(N_3)-Me** 2.25, **4Ni(CN)-Me** 2.95 (under TBA peak), **2Ni-Me** 1.94) (Figure 8). These results corroborate the interplay between the electronics of the small molecule and the N-functionalized pyridine by looking at the chemical shift of the *H*-C1 proton.

Overall the crystal structures reported here indicate that the interactions of Ni^0 and Pd^0 with aromatic π-systems become stronger upon changing the pendant donor from benzene to pyridine to Lewis acid functionalized pyridine. This trend is maintained upon binding of additional ligands such CO. The electronic effect of these interactions with pendant π-systems is reflected in extent of CO bond weakening. The metal pyridine π-system interaction can also be modulated with the π-acidity of coordinated ligand.

Section 4.4 Pyridine Dearomatization by Small Molecule Reactivity

With the influence of the aromatic ligand on the metal center demonstrated, the activation of the heterocycle by the metal toward reactivity was also investigated. With the aromaticity of pyridine partially disrupted by metal coordination, reactivity at the N=C moiety was targeted. **2Ni** showed no reactivity under an atmosphere of dihydrogen at room temperature in benzene, and increasing the temperature was found to yield free phosphine, **1**, presumably with loss of nickel black. However, reactions with pinacol borane and phenylsilane led to the formation of new species, **6Ni** and **7Ni**, respectively, at room temperature by NMR spectroscopy (Scheme 5).

Attempts to obtain X-ray diffraction quality single crystal of **6Ni** and **7Ni** have been unsuccessful to date. A suite of NMR experiments were employed for the structural characterization of these compounds. Both complexes show asymmetric coupling ^{31}P doublets at (56.23, 44.70 ppm ($^2J_{PP}$ = 55.7 Hz)) and (56.09, 44.77 ($^2J_{PP}$ = 56.2)) for **6Ni** and **7Ni,** respectively. Furthermore, asymmetric signals for the central pyridine protons are observed that are consistent with the hydroboration or hydrosilylation of a C–N bond of the pyridine rather than a 1,4 selective reaction or a formal oxidative addition at the nickel center. The formation of a methylene moiety with diastereotopic hydrogens is supported by two doublet proton resonances for **6Ni** (4.51, 3.78 ppm ($^2J_{HH}$ = 13.7 Hz)) and **7Ni** (4.13, 3.77 ppm ($^2J_{HH}$

= 13.2 Hz)) are correlated by gCOSY and couple to the same ^{13}C resonance at 52.40 or 55.15 ppm, respectively, by gHSQCAD. The assignments for the remaining central pyridine protons are completed using a combination of gHSQCAD and gHMBCAD experiments, which confirm the location of the C1 and the remaining *ortho*-pyridine protons at 4.11 and 6.83 ppm and 4.13 and 6.40 ppm for **6Ni** and **7Ni** respectively (Figure 9). The Si*H* signal of **7Ni** appears as a multiplet at 5.29 ppm. Complete assignments of the central pyridine carbons have also been made (See Experimental Section), which support the 1,2 substitution pattern assignment.

Scheme 5. Reactivity at pyridine beyond Lewis acid binding: synthesis of dearomatized pyridine complexes

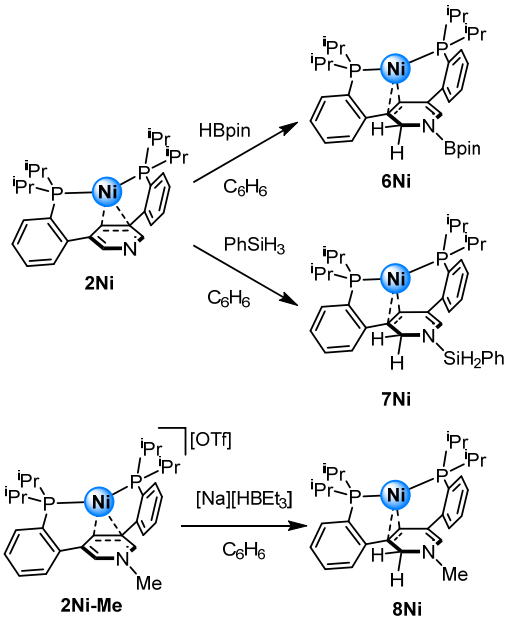

To further support the NMR-based structural assignments for **6Ni** and **7Ni**, the reactivity of hydrides with **2Ni-Me** was tested to determine if a similar dearomatization occurs. **2Ni-Me** was found to cleanly react with sodium triethylborohydride to yield the asymmetric species **8Ni**. Similar to **6Ni** and **7Ni** coupling ^{31}P doublets are seen at 56.52 and 44.05 ppm ($^{2}J_{PP}$ = 56.4 Hz). The pattern of ^{1}H resonances and the connectivity of the dearomatized central pyridine ring was found to be similar to that of **6Ni**. The methylene protons are observed at

3.49 and 3.09 ppm ($^{2}J_{HH}$ = 12.0 Hz), while the C1 and remaining *ortho*-pyridine proton are observed at 4.09 and 5.85 ppm respectively.

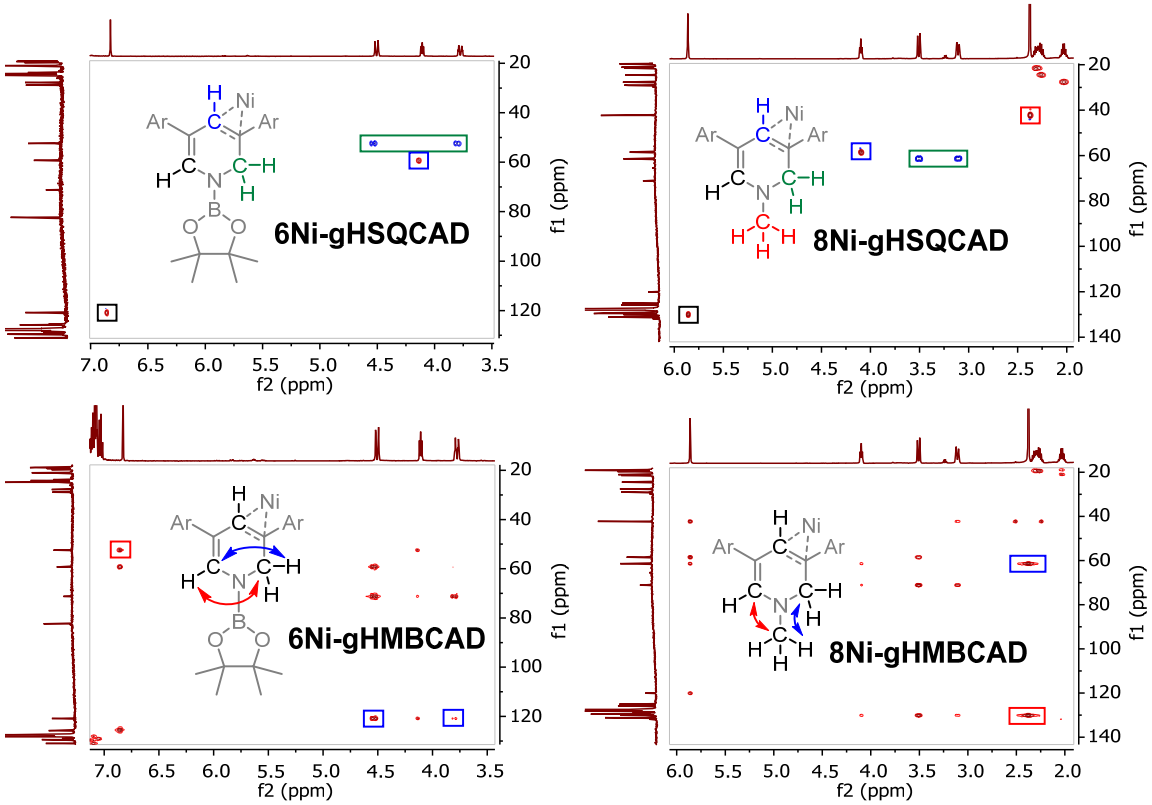

Figure 9. Select portions of the gHSQCAD and gHMBCAD spectra for **6Ni** (Left) and **8Ni** (Right).

Complexes **6Ni**, **7Ni**, and **8Ni** are reminiscent of transition metal bound NAD(P)H analogs.[17] The use of pyridine and other heterocycles to store proton and electron equivalents in metal-complexes has been previously explored for a variety of transformations.[18] In the context of π-bound ligands, catechol moieties have been shown to act as a source of both electrons and electrophile equivalents during dioxygen activation.[19] **6Ni**, **7Ni**, and **8Ni** demonstrate the ability of the pyridine to serve as a reservoir of reducing equivalents in the present system. Access to these reduced species is however sensitive to the steric and electronic properties of the reagents. Diphenylsilane and triethylsilane did not react with **2Ni** even at

elevated temperatures. The addition of sodium triethylborohydride to **2Ni-BCy$_2$OTf** did not result in the formation of a dearomatized product by ^{31}P NMR. Although the final products **6Ni**, **7Ni**, and **8Ni** show delivery of hydride to the pyridine, mechanistically the initial site of reactivity, metal vs heterocycle, has not been established. A precise understanding of the factors that govern the pyridine reduction reactivity require further investigation, as do methodologies to transfer the reducing equivalents to an external substrate.

Section 4.5 Preliminary Mo Metalation Reactions

Preliminary attempts have been made to expand the scope of metals supported by ligands **1** and **1-B(C$_6$F$_5$)$_3$** beyond Ni and Pd. Initials efforts focused on metalation conditions with molybdenum carbonyl precursors as such compounds have served as precursors for a variety of compounds capable of interesting multielectron transformations on *para*-terphenyl diphosphine ligands.[19-20] The stirring of **1** with Mo(CO)$_3$(MeCN)$_3$ at 100 °C for 16 hours in toluene produced a major species at 55.17 ppm (~80 %) and a minor species at 55.89 ppm (~20 %). Efforts to separate these complexes with solvent washes or by recrystallization proved unsuccessful. However, protonation of this mixture with pyridinium triflate and recrystallization was sufficient to cleanly afford **9Mo(CO)$_3$-H** (Scheme 6). To date to decarbonylate or oxidize **9Mo(CO)$_3$-H** have proven unsuccessful. The reaction with trimethylamine *n*-oxide was found to cleanly afford the deprotonation product, **9Mo(CO)$_3$**, which could then be identified as the major species in the initial metalation of **1** with Mo(CO)$_3$(MeCN)$_3$. The current hypothesis is that the minor species is dimolybenum complex where the pyridine nitrogen coordinates to a second metal. The metallation of **1-B(C$_6$F$_5$)$_3$** with Mo(CO)$_3$(MeCN)$_3$ under identical reaction conditions produces a single new species, **9Mo(CO)$_3$-B(C$_6$F$_5$)$_3$**, consistent with the aforementioned hypothesis as boron

prefunctionalization of the pyridine nitrogen would prevent the formation of the proposed dimolybdenum species.

Scheme 6. Synthesis of molybdenum carbonyl complexes supported by 1 and 1-B(C_6F_5)$_3$

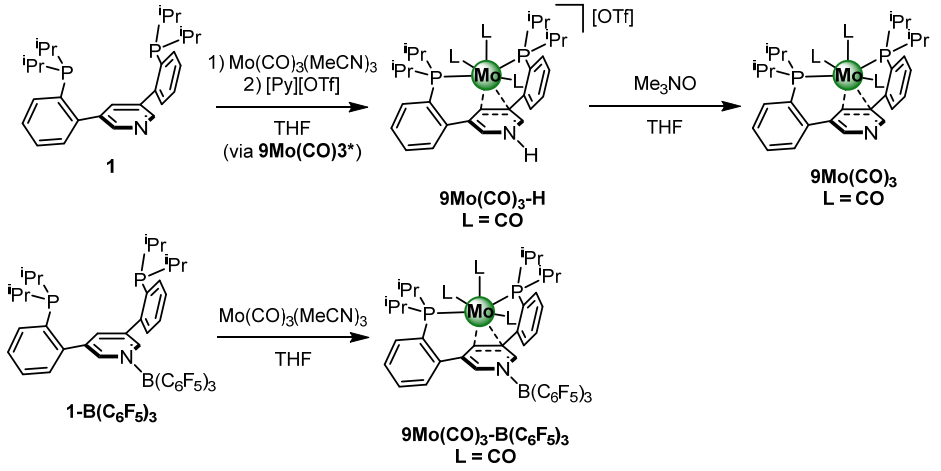

Solution NMR data obtained for **9Mo(CO)$_3$** and **9Mo(CO)$_3$-B(C$_6$F$_5$)$_3$** (C_6D_6) as well as **9Mo(CO)$_3$-H** (CD_3CN) are consistent with strong metal-pyridine π-system interactions and a C_s symmetric species or a fluxional process on the NMR timescale. All compounds show a pair of resonances corresponding to the methine protons (δ(ppm): **9Mo(CO)$_3$** (2.67, 2.36), **9Mo(CO)$_3$-B(C$_6$F$_5$)$_3$** (2.48, 2.05), **9Mo(CO)$_3$-H** (3.31, 2.58)) and a single ^{31}P signal (δ(ppm): **9Mo(CO)$_3$** 55.17, **9Mo(CO)$_3$-B(C$_6$F$_5$)$_3$** 55.97, **9Mo(CO)$_3$-H** 54.63). The ^{1}H resonances for the central pyridine protons appear at upfield resonances compared to the free ligands (*H*-(C1) δ(ppm): **9Mo(CO)$_3$** 6.15, **9Mo(CO)$_3$-B(C$_6$F$_5$)$_3$** 4.97, **9Mo(CO)$_3$-H** 5.35) (*H*-(C3/4) δ(ppm): **9Mo(CO)$_3$** 8.39, **9Mo(CO)$_3$-B(C$_6$F$_5$)$_3$** 8.11, **9Mo(CO)$_3$-H** 7.96). These data suggest that a substantial Mo-pyridine π-system interaction which is stronger for the more electron deficient B(C_6F_5)$_3$- and H^+-functionalized central pyridine ring. **9Mo(CO)$_3$-H** shows a broad ^{1}H signal corresponding to the pyridinium resonance at 12.37 ppm.

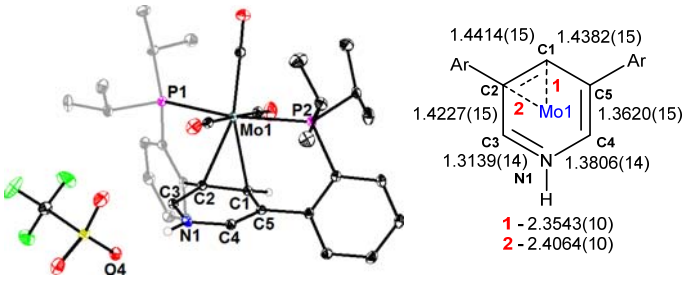

Figure 10. Solid-state structures and selected bond distances for **9Mo(CO)$_3$-H**. Hydrogen atoms and solvent have been omitted for clarity.

Crystals of **9Mo(CO)$_3$-H** suitable for XRD analysis were obtained from a THF/pentane vapor diffusion (Figure 10). A *pseudo*-octahedral coordination environment around the Mo-center is observed, which shows η^2 coordination to the central pyridine ring. Substantial backbonding from Mo is evident from the long C1–C2 bond distance (1.4414(15) Å), which exceeds that of all other C–C bonds in the pyridine ring. The alternation of long and short bonds in the central pyridine ring is indicative of localization of double bond character due to Mo coordination. Efforts to open up the coordination sphere of the Mo center by removing the carbon monoxide ligands is being pursued.

CONCLUSIONS

A new P-pyridine-P ligand that readily binds nickel and palladium via phosphine donors and the heterocycle π-system was developed. The interaction between the transition metal and the π-system results in partial disruption of aromaticity. Metal coordination to the phosphine donors and pyridine π-system leaves the pyridine nitrogen available for Lewis acid functionalization. Binding of groups such as boranes, H^+, or Me^+ results in stronger interactions of the metal center with the pyridine π-

system, as reflected in both the NMR spectroscopy and structural characteristics of the complexes. The observed differences in binding are caused by the varied ability of pyridines to act as π-backbonding ligands; the functionalized heterocycles are more electron-deficient resulting in a stronger interaction with the electron rich M^0 centers. CO and NO adducts of Ni were synthesized. Comparison of the CO stretching frequencies indicate that functionalization of the pyridine nitrogen has a significant effect on the coordinated diatomic ligand, leading to up to 46 cm^{-1} shift to higher energy upon $B(C_6F_5)_3$ binding. Dearomatization of the pyridine ring was observed in stoichiometric reactions between phenylsilane or pinacol borane and **2Ni**, with the heteroatom binding to nitrogen and the hydrogen *ortho* to N. This ligand-based reactivity is likely a consequence of the activation of the pyridine ring by the metal center, through disruption of aromaticity. Overall, the described results highlight a strategy for tuning the electronic properties and reactivity of metal centers by post-synthetic modifications of the complex instead of the more typical, and expensive, re-synthesis of electronically altered ligands.

EXPERIMENTAL SECTION

General considerations

Unless otherwise specified, all air- and moisture-sensitive compounds were manipulated using glovebox or using standard Schlenk line techniques with an N_2 atmosphere. Anhydrous tetrahydrofuran (THF) was purchased from Aldrich in 18 L Pure-Pac™ containers. Anhydrous pentanes, hexanes, benzene, toluene, diethyl ether, and THF were purified by sparging with nitrogen for 15 minutes and then passing under nitrogen pressure through a column of activated A2 alumina (Zapp's).[21] Benzene-d_6, tetrahydrofuran-d_8, and acetonitrile-d_3 was purchased from Cambridge Isotope Laboratories, Inc., dried over sodium/benzophenone ketyl (benzene and THF) or calcium hydride (MeCN) and vacuum transferred prior to use. Unless indicated otherwise, all commercial chemicals were used as received. $Ni(COD)_2$, $PdMe_2$TMEDA, $PdCl_2$COD, and $Pd(PPh_3)_4$ were purchased from Strem Chemicals Inc.. 3,5-dibromopyridine, pinacol borane, dicyclohexylboron triflate, methyl triflate, 1M sodium triethylborohydride in toluene, 1.7 M *t*BuLi in pentane, chlorodiisopropyl phosphine, and CO (lecture bottle) was purchased from Sigma Aldrich. Phenylsilane was purchased from Sigma Alrich and was dried over calcium hydride and distilled prior to use. Tris(pentafluorophenyl)borane was purchased from Sigma Aldrich as sublimed prior to use. 2-bromophenylboronic acid was purchased from Ark Pharm, Inc. and used as received. ^{1}H, ^{13}C, and ^{31}P NMR spectra were recorded on Varian Mercury 300 or Varian INOVA-500 spectrometers at room temperature unless indicated otherwise. Chemical shifts for ^{1}H and ^{13}C NMR data are reported relative to residual solvent peaks and are decoupled with respect to each other unless otherwise noted.[22] ^{31}P NMR chemical shifts are reported with respect to the deuterated solvent used to lock the instrument and are ^{1}H decoupled unless otherwise noted. Powder and thin film ATR-IR measurements were obtained by placing a powder or drop of

solution of the complex on the surface of a Bruker APLHA ATR-IR spectrometer probe and allowing the solvent to evaporate (Platinum Sampling Module, diamond, OPUS software package) at 2 cm^{-1} resolution. Elemental analyses were performed by Robertson Microlit Laboratories, Ledgewood, NJ.

Synthesis of 3,5-(2-bromophenyl)pyridine (B)

3,5-dibromopyridine (8.50 g, 35.9 mmol, 1 equiv), 2-bromophenylboronic acid (15.13 g, 75.3 mmol, 2.1 equiv), and potassium carbonate (29.8 g, 215.6 mmol, 6 equiv) were added to a Schlenk tube fitted with a screw-in Teflon stopper. A magnetic stirbar, 810 mL of toluene, 195 mL of water, and 195 mL of ethanol were then added the resulting biphasic solution was thoroughly degassed by two sequential freeze-pump-thaw cycles on a Schlenk line. Under a strong counterflow of nitrogen, $Pd(PPh_3)_4$ (2.07 g, 1.79 mmol, 0.05 equiv) was then added to the reaction mixture. The reaction flask was then sealed and heated to 65 °C for 16 hrs. At this point, GC-MS analysis of an aliquot of the organic fraction indicated complete conversion to the desired product. Volatiles were removed by rotary evaporation to yield a light orange residue. Salts were removed by a water:dichloromethane extraction. After drying with magnesium sulfate and filtering, the organic fraction was dried under reduced pressure. The product was recrystallized from dichloromethane:methanol at -35 °C and obtained as a white crystalline solid. Yield: 7.93 g (59 %) ^{1}H NMR (500 MHz, C_6D_6) δ 8.75 (d, $^4J_{HH}$ = 2.2 Hz, Py*H*, 2H), 7.51 (t, $^4J_{HH}$ = 2.2 Hz, Py*H*, 1H), 7.40 (ddd, $^3J_{HH}$ = 8.0, $^4J_{HH}$ = 1.2, $^5J_{HH}$ = 0.5 Hz, Ar*H*, 2H), 6.92 (ddd, $^3J_{HH}$ = 7.6, $^4J_{HH}$ = 1.9, $^5J_{HH}$ = 0.5 Hz, Ar*H*, 2H), 6.87 (td, $^3J_{HH}$ = 7.5, $^4J_{HH}$ = 1.2 Hz, Ar*H*, 2H), 6.72 (ddd, $^3J_{HH}$ = 8.0, $^3J_{HH}$ = 7.3, $^4J_{HH}$ = 1.8 Hz, Ar*H*, 2H). ^{13}C NMR (126 MHz, C_6D_6) δ 149.52 (s), 139.37 (s), 137.50 (s), 136.08 (s), 133.51 (s), 131.65 (s), 129.63 (s), 127.71 (s), 123.2 4 (s). MS (m/z): Calcd, 389.9316 (M^+). Found: 389.9327 (FAB-MS, M^+).

Synthesis of Compound 1

B (4 g, 10.3 mmol, 1 equiv) was dissolved in 60 mL of THF and transferred to a Schlenk tube fitted with a screw-in Teflon stopper. The reaction mixture was then cooled to -78 °C and then *t*BuLi (1.7 M pentanes, 24.8 mL, 42.2 mmol, 4.1 equiv) was added via syringe resulting in an immediate color change to a deep red. The reaction mixture was then allowed to warm to room temperature and stir for 2 hrs. The reaction mixture was again cooled to -78 ºC and then chlorodiisopropyl phosphine (3.6 mL, 22.6 mmol, 2.2 equiv) was added via syringe. The reaction was warmed to room temperature and allowed to stir for 16 hrs during which time the solution lightened to a homogenous orange brown. Volatiles were then removed under reduced pressure to yield a thick residue. This residue was dissolved in toluene a filtered through a Celite pad to remove salts. The volatiles of the filtrate were then removed under reduced pressure. The resulting residue was suspended in acetonitrile (*ca.* 20 mL) and then resulting solution allowed to stand for 1 hour. During this time the residue initially became soluble before the product began to precipitate as a yellow solid. This product was collected via filtration and washed with additional acetonitrile until the washes became colorless. After drying the collected solid under reduced pressure, the product was obtained as a pale yellow solid. Yield: 2.82 g (59 %). ^{1}H NMR (500 MHz, C_6D_6) δ 8.94 (dd, $^{3}J_{HH}$ = 2.2 Hz, $^{5}J_{PH}$ = 1.3 Hz, Py*H*, 2H), 7.87 (td, $^{3}J_{HH}$ = 2.2 Hz, $^{5}J_{PH}$ = 1.1 Hz, Py*H*, 1H), 7.45 – 7.36 (m, Ar*H*, 2H), 7.35 – 7.27 (m, Ar*H*, 2H), 7.15 – 7.09 (m, Ar*H*, 4H), 1.86 (pd, $^{3}J_{HH}$ = 6.9, $^{2}J_{PH}$ =1.6 Hz, C*H*, 4H), 0.95 (dd, $^{3}J_{PH}$ = 14.6, $^{3}J_{HH}$ =6.9 Hz, C*H*$_3$, 12H), 0.85 (dd, $^{3}J_{PH}$ = 11.5, $^{3}J_{HH}$ = 6.9 Hz, C*H*$_3$, 12H). ^{13}C NMR (126 MHz, C_6D_6) δ 150.33 (d, $^{5}J_{PC}$ = 5.9 Hz), 147.55 (d, $^{2}J_{PC}$ = 28.3 Hz), 140.29 (t, $^{5}J_{PC}$ = 4.9 Hz), 137.11 (d, $^{3}J_{PC}$ = 6.2 Hz), 135.64 (d, $^{1}J_{PC}$ = 24.6 Hz), 133.04 (d, $^{2}J_{PC}$ = 2.9 Hz), 130.96 (d, $^{3}J_{PC}$ = 5.4 Hz), 129.01 (s), 127.42 (s), 25.01 (d, $^{1}J_{PC}$ = 15.6 Hz), 20.47 (d, $^{2}J_{PC}$ =

20.2 Hz), 19.75 (d, $^{2}J_{PC}$ = 11.0 Hz). ^{31}P NMR (121 MHz, C_6D_6) δ -5.75. MS (m/z): Calcd, 464.2638 (M+). Found: 464.2636 (FAB-MS, M^+).

Synthesis of Complex 1-B(C_6F_5)$_3$

Compound **1** (562 mg, 1.21 mmol, 1 equiv.) was dissolved in benzene (*ca.* 10 mL) and transferred to a 20 mL scintillation vial equipped with a magnetic stirbar. B(C_6F_5)$_3$ (620.7 mg, 1.21 mmol, 1 equiv.) was then added as a benzene solution (*ca.* 10 mL). The reaction mixture was allowed to stir for 3 hours, during which time the solution became a slightly lighter shade of yellow. The reaction mixture was then frozen in a -35 °C freezer and the benzene removed by lyophilization to yield the desired product by NMR and was used without further purification. Yield: 1.06 g (90 %) ^{1}H NMR (500 MHz, C_6D_6) δ 8.82 (s, Py*H*, 2H), 8.04 (s, Py*H*, 1H), 7.26 – 7.18 (m, Ar*H*, 4H), 7.08 – 6.97 (m, Ar*H*, 4H), 1.70 (pd, $^{1}J_{HH}$ = 6.9, $^{1}J_{PH}$ = 2.3 Hz, C*H*, 4H), 0.82 (dd, $^{2}J_{PH}$ = 14.6, $^{1}J_{HH}$ = 6.9 Hz, C*H*$_3$, 12H), 0.72 (dd, $^{2}J_{PH}$ = 12.3, $^{1}J_{HH}$ = 6.9 Hz, C*H*$_3$, 12H). ^{13}C NMR (126 MHz, C_6D_6) δ 149.20 (s), 147.97 – 146.77 (m), 145.99 (d, $^{5}J_{PC}$ = 7.0 Hz), 142.87 (d, $^{2}J_{PC}$ = 26.8 Hz), 141.22 (m), 139.65 – 138.95 (m), 139.18 (d, $^{3}J_{PC}$ = 5.7 Hz), 136.37 (m), 134.65 (d, $^{1}J_{PC}$ = 25.1 Hz), 132.83 (d, $^{2}J_{PC}$ = 2.4 Hz), 130.22 (d, $^{4}J_{PC}$ = 5.3 Hz), 129.35 (s), 128.76 (s), 128.17 (s), 23.68 (d, $^{1}J_{PC}$ = 13.6 Hz), 19.23 (d, $^{2}J_{PC}$ = 18.1 Hz), 18.93 (d, $^{2}J_{PC}$ = 11.4 Hz). ^{31}P NMR (121 MHz, C_6D_6) δ -5.58. ^{19}F NMR (282 MHz, C_6D_6) δ -131.46 (s), -155.96 (s), -162.87 (s). MS (m/z): Calcd, 976.2484 (M+). Found: 976.2389 (FAB-MS, M+).

Synthesis of Complex 2Ni

Compound **1** (1.00 g, 2.15 mmol, 1 equiv.) was transferred as a tetrahydrofuran solution (*ca.* 20 mL) into a Schlenk flask fitted with a screw-in Teflon stopper and equipped with a magnetic stirbar. Ni(COD)$_2$ (593.3 mg, 2.15 mmol, 1 equiv.) was then added as a

tetrahydrofuran suspension (*ca.* 20 mL). The reaction mixture was then sealed and allowed to stir for 16 hrs, during which time to solution changed color from a yellow to a dark red brown. All volatiles were then removed under reduced pressure. The residue was then dissolved in benzene and filtered through a Celite pad. The volatiles of the filtrate were removed under reduced pressure to yield the product as a dark brown clumpy solid. Yield: 833 mg (74 %) ^{1}H NMR (300 MHz, C_6D_6) δ 7.82 (broad s, Py*H*, 2H), 7.47 (d, J = 6.9 Hz, Ar*H*, 2H), 7.22 (d, J = 6.0 Hz, Ar*H*, 2H), 7.10 (m, Ar*H*, 4H), 4.35 (s, Py*H*, 1H), 2.28 (m, C*H*, 2H), 2.07 (m, C*H*, 2H), 1.07 (m, C*H*$_3$, 7.6 Hz, 18H), 0.91 (m, C*H*$_3$, 6H). ^{13}C NMR (126 MHz, C_6D_6) δ 150.84 (s), 142.31 (s), 136.58 (s), 132.64 (s), 129.12 (s), 128.42 (s), 128.19 (s), 106.12 (s), 59.21 (s), , 27.02 (s), 24.61 (d, $^{1}J_{PC}$ = 15.6 Hz), 22.27 (s), 20.07 (d, $^{1}J_{PC}$ = 20.1 Hz), 19.25 (s). ^{31}P NMR (121 MHz, C_6D_6) δ 40.38 (s). Anal. Calcd. for: $C_{29}H_{39}NP_2Ni$ (**2Ni**) (%): C, 66.69; H, 7.53; N, 2.68. Found: C, 65.15; H, 6.89; N, 2.21.

Synthesis of Complex 2Pd

Compound **1** (211.9 mg, 0.457 mmol, 1 equiv.) was transferred as a benzene solution (*ca.* 10 mL) into a Schlenk flask fitted with a screw-in Telfon stopper and equipped with a magnetic stirbar. $PdMe_2$(TMEDA) (127.05 mg, 0.503 mmol, 1.1 equiv.) was then added as a benzene suspension (*ca.* 20 mL). The reaction mixture was then sealed and heated to 60 °C for 16 hrs, during which time the reaction changed color from yellow to a bright orange. The solution was then filtered through a Celite pad, and the volatiles of the resulting filtrate were removed under reduced pressure to yield clean product as an orange solid without further purification. Yield: 197.6 mg (76 %). ^{1}H NMR (500 MHz, C_6D_6) δ 8.29 (s, Py*H*, 2H), 7.90 (s, Py*H*, 1H), 7.24 (m, Ar*H*, 4H), 7.15 – 7.10 (m, Ar*H*, 2H), 7.05 (m, Ar*H*, 2H), 2.22 – 2.01 (m, C*H*, 2H), 1.86 (p, $^{3}J_{HH}$ = 7.2 Hz, C*H*, 2H), 1.28 (dd, $^{3}J_{PH}$ = 7.8, $^{3}J_{HH}$ = 7.6 Hz, C*H*$_3$, 6H), 1.08 (dd, $^{3}J_{PH}$ =

8.0, $^{3}J_{HH}$ =7.5 Hz, C*H*$_3$, 6H), 0.96 (dd, $^{3}J_{PH}$ = 7.9, $^{3}J_{HH}$ = 7.7 Hz, C*H*$_3$, 6H), 0.73 (dd, $^{3}J_{PH}$ = 5.9, $^{3}J_{HH}$ = 5.8 Hz, C*H*$_3$, 6H). ^{13}C NMR (126 MHz, C_6D_6) δ 147.39 (vt, $^{2}J_{PC}$ = 11.1 Hz), 146.18 (s), 134.51 (vt, $^{1}J_{PC}$ = 13.6 Hz), 131.64 (s), 131.44 (vt, $^{3}J_{PC}$ =5.0 Hz), 130.68 (s), 128.61 (s), 127.24 (s), 105.30 (s), 27.87 (vt, $^{2}J_{PC}$ = 5.7 Hz), 21.75 (vt, $^{2}J_{PC}$ = 7.8 Hz), 20.66 (vt, $^{3}J_{PC}$ = 5.5 Hz), 17.07 (s). ^{31}P NMR (121 MHz, C_6D_6) δ 33.76 (s). Anal. Calcd. for: $C_{29}H_{39}NP_2Pd$ (**2Pd**) (%): C, 61.11; H, 6.90; N, 2.46. Found: C, 60.87; H, 6.70; N, 2.45.

Synthesis of Complex 2Ni-B(C_6F_5)$_3$

Compound **1-B(C_6F_5)$_3$** (126.7 mg, 0.129 mmol, 1 equiv.) was transferred as a benzene solution (*ca.* 10 mL) into a Schlenk flask fitted with a screw-in Telfon stopper and equipped with a magnetic stirbar. Ni(COD)$_2$ (35.7 mg, 0.129 mmol, 1 equiv.) was then added as a benzene suspension (*ca.* 10 mL). The reaction was allowed to stir for 16 hrs, during which time the solution changed color from a pale yellow to dark brown. The volatiles were then removed under reduced pressure. The brown residue was then dissolved in benzene and filtered through a Celite pad. The volatiles of the filtrate were removed under reduced pressure to yield the product as a dark brown solid. Yield: 94 mg (70 %) ^{1}H NMR (500 MHz, C_6D_6) δ 7.42 (d, J_{HH} = 7.0 Hz, Ar*H*, 2H), 7.37 (s, Py*H*, 2H), 7.01 (m, Ar*H*, 2H), 7.00 – 6.94 (m, Ar*H*, 2H), 3.18 (s, Py*H*, 1H), 2.07 (m, C*H*, 2H), 1.85 – 1.70 (m, C*H*, 2H), 0.88 (dd, $^{3}J_{PH}$ = 14.7, $^{3}J_{HH}$ = 7.5 Hz, C*H*$_3$, 6H), 0.85 – 0.77 (m, 18H). ^{13}C NMR (126 MHz, C_6D_6) δ 149.07 (s), 147.45 (vt, $^{2}J_{PC}$ = 10.9 Hz), 147.15 (s), 140.72 (s), 138.74 (s), 138.19 (s), 136.30 (m), 135.93 – 135.32 (m), 135.07 (s), 131.77 (d, $^{3}J_{PC}$ = 7.3 Hz), 131.13 (s), 130.48 (s), 130.09 – 129.14 (m), 128.89 (s), 128.61 (s), 119.66 (s), 104.74 (s), 49.97 – 47.80 (m), 28.42 – 26.47 (m), 22.26 – 20.89 (m), 20.15 – 18.18 (m). ^{31}P NMR (121 MHz, C_6D_6) δ 41.97 (s). ^{19}F NMR (282 MHz, C_6D_6) δ -131.42 (s), -157.56

(s), -163.95 (s). Anal. Calcd. for: $C_{47}H_{39}BF_{15}NP_2Ni$ (**2Ni-B(C_6F_5)$_3$**) (%): C, 54.48; H, 3.80; N, 1.35. Found: C, 55.71; H, 3.79; N, 1.28.

Synthesis of Complex 2Pd-B(C_6F_5)$_3$

Compound **1-B(C_6F_5)$_3$** (110.3 mg, 0.113 mmol, 1 equiv.) was dissolved in tetrahydrofuran (*ca.* 5 mL) and transferred to a 20 mL scintillation vial equipped with a magnetic stirbar. $PdCl_2COD$ (32.3 mg, 0.113 mmol, 1 equiv.) was then added as a suspension in tetrahydrofuran (*ca.* 5 mL). The reaction mixture was allowed to stir for 3 hrs, during which time the solution changed color from a yellow suspension to a homogeneous orange color. Ni(bpy)(COD) (36.5 mg, 0.113 mmol, 1 equiv.) was then added as a tetrahydrofuran solution (*ca.* 10 mL) resulting in an immediate color change from orange to a pink purple solution heterogeneous solution. The reaction mixture was allowed to stir for 30 mins before filtering through a Celite pad. The volatiles of the filtrate were then removed under reduced pressure to yield a pink purple solid. Yield: 96.7 mg (79 %). ^{1}H NMR (500 MHz, C_6D_6) δ 7.69 (s, Py*H*, 2H), 7.47 (s, Ar*H*, 2H), 7.09 – 7.04 (m, Ar*H*, 4H), 7.01 (m, Ar*H*, 2H), 6.39 (s, Py*H*, 1H), 2.02 (m, C*H*, 2H), 1.69 (p, $^3J_{HH}$ = 7.0 Hz, C*H*, 2H), 1.03 (dd, $^3J_{PH}$ = 8.0, $^3J_{HH}$ = 7.7 Hz, C*H*$_3$, 6H), 0.88 (dd, $^3J_{PH}$ = 7.9, $^3J_{HH}$ =7.8 Hz, C*H*$_3$, 6H), 0.78 (q, $^3J_{PH}$ = 7.9, $^3J_{HH}$ = 7.8 Hz, C*H*$_3$, 6H), 0.66 (dd, $^3J_{PH}$ =J = 6.5, $^3J_{HH}$ = 6.2 Hz, C*H*$_3$, 6H). ^{13}C NMR (126 MHz, C_6D_6) δ 148.97 (s), 147.04 (s), 145.25 (t), 140.80 (s), 138.81 (s), 138.22 (s), 138.00 (s), 136.37 (s), 131.56 (t, J = 16.5 Hz), 131.51 (s), 130.35 (s), 130.07 (s), 128.63 (s), 126.81 (t, J = 6.1 Hz), 120.10 (s), 86.87 (s), 27.80 (vt, $^2J_{PC}$ = 6.9 Hz), 21.32 (vt, $^3J_{PC}$ = 9.0 Hz), 19.77 (vt, $^3J_{PC}$ = 6.9 Hz), 19.30 (m), 17.22 (s). ^{31}P NMR (121 MHz, C_6D_6) δ 34.06 (s). ^{19}F NMR (282 MHz, C_6D_6) δ -131.04 (s), -157.36 (s), -163.73 (s). Anal. Calcd. for: $C_{47}H_{39}BF_{15}NP_2Pd$ (**2Pd-B(C_6F_5)$_3$**) (%): C, 52.17; H, 3.63; N, 1.29. Found: C, 51.80; H, 3.69; N, 1.71.

Synthesis of Complex 2Ni-Me

Compound **2Ni** (213 mg, 0.408 mmol, 1 equiv.) was dissolved in benzene (*ca.* 12 mL) and transferred to a 20 mL scintillation vial equipped with a magnetic stirbar. MeOTf (44.7 μL, 0.408 mmol, 1 equiv.) was added by Hamilton syringe to a rapidly stirring reaction mixture, which resulted in a color change from red brown to a darker brown. After stirring for 30 mins, volatiles were then removed under reduced pressure to yield the desired product as a dark brown solid without the need for further purification. Yield: 260 mg (93 %). ^{1}H NMR (300 MHz, C_6D_6) δ 7.25 – 7.18 (m, Ar*H*, 2H), 7.16 – 7.11 (m, Ar*H*, 4H), 7.10 – 7.01 (m, Ar*H*, 2H), 6.78 – 6.73 (m, Py*H*, 2H), 2.77 (t, $^{4}J_{HH}$ = 1.4 Hz, NC*H*$_3$, 3H), 2.57 (m, C*H*, 2H), 2.45 (m, C*H*, 2H), 1.99 – 1.90 (t, $^{2}J_{PH}$ = 5.0 Hz, 1H), 1.22 – 1.13 (m, C*H*$_3$, 6H), 1.13 – 1.06 (m, C*H*$_3$, 6H), 1.06 – 0.99 (m, C*H*$_3$, 6H), 0.99 – 0.91 (m, C*H*$_3$, 6H). ^{13}C NMR (126 MHz, C_6D_6) δ 147.30 (s), 133.92 (s), 131.41 (s), 129.38 (s), 129.18 (s), 128.52 (s), 128.42 (s), 128.19 (s), 104.91 (s), 44.95 (s), 41.69 (s), 26.42 (s), 23.30 (s), 19.43 (s), 18.97 (s), 18.65 (s), 18.38 (s). ^{31}P NMR (121 MHz, C_6D_6) δ 31.13 (s). ^{19}F NMR (282 MHz, C_6D_6) δ -77.43 (s). Anal. Calcd. for: $C_{31}H_{42}F_3NNiO_3P_2S$ (**2Ni-Me**) (%): C, 54.25; H, 6.17; N, 2.04. $C_{37}H_{48}F_3NNiO_3P_2S$ (**2Ni-Me·(C_6H_6)**) (%): C, 58.13; H, 6.33; N, 1.83. Found: C, 57.24; H, 6.01; N, 1.70.

Synthesis of Complex 2Ni-BCy$_2$OTf

Compound **2Ni** (113.4 mg, 0.217 mmol, 1 equiv.) was dissolved in benzene (*ca.* 5 mL) and transferred to a 20 mL scintillation vial equipped with a magnetic stirbar. Dicyclohexylboron triflate (70.8 mg, 0.217 mmol, 1 equiv.) was added as a benzene solution (*ca.* 5 mL), which resulted in an immediate color change from red brown to a dark green solution before gradually turning a dark brown similar to that of **2Ni-B(C_6F_5)$_3$**. The solution was allowed to stir for 3 hrs before volatiles were removed under reduced pressure yielding the desired

complex as a dark brown solid without the need for further purification. Yield: 120 mg (65 %). ^{1}H NMR (300 MHz, C_6D_6) δ 7.43 (s, Py*H*, 2H), 7.41 (s, Ar*H*, 2H), 7.11 – 7.00 (m, Ar*H*, 6H), 3.45 (s, Py*H*, 1H), 2.33 (s, 2H), 2.13 (m, 1H), 2.00 – 1.80 (m, 8H), 1.71 (s, 1H), 1.43 (m, 10H), 1.30 (m, 2H), 1.10 – 0.99 (m, 6H), 0.97 – 0.81 (m, 18H). ^{13}C NMR (126 MHz, C_6D_6) δ 147.86 (s), 142.37 (s), 136.04 (s), 133.94 (s), 131.16 (s), 130.29 (s), 104.49 (s), 29.29 (s), 28.83 (s), 28.15 (s), 27.74 (s), 27.41 (s), 27.02 (s), 21.40 (s), 19.71 (s), 18.79 (s). ^{31}P NMR (121 MHz, C_6D_6) δ 42.29. ^{19}F NMR (282 MHz, C_6D_6) δ -77.35.

Synthesis of Complex 2Pd-H

Compound **2Pd** (34.7 mg, 0.0609 mmol, 1 equiv.) was dissolved in tetrahydrofuran (*ca.* 4 mL) and transferred to a 20 mL scintillation vial equipped with a magnetic stirbar. Pyridinium triflate (13.95 mg, 0.0609 mmol, 1 equiv.) was then added as a tetrahydrofuran solution (*ca.* 4 mL). This resulted in an immediate color change from orange to a bright pink solution. The reaction mixture was allowed to stir for 1 hr before all volatiles were removed under reduced pressure to yield clean product as a pink solid without further purification. Yield: 40.3 mg (92 %) ^{1}H NMR (500 MHz, CD_3CN) δ 9.88 (s, PyN*H*, 1H), 7.75 – 7.66 (m, Ar*H*, 2H), 7.66 – 7.54 (m, Ar*H*, 4H), 7.47 – 7.36 (m, Ar*H*, 2H), 7.28 (s, Py*H*, 2H), 6.16 (s, Py*H*, 1H), 2.77 (m, C*H*, 2H), 2.30 (m, C*H*, 2H), 1.28 (dd, $^{3}J_{PH}$ = 9.2, $^{3}J_{HH}$ = 6.9 Hz, C*H*$_3$, 6H), 1.15 (dd, $^{3}J_{PH}$ = 8.8, $^{3}J_{HH}$ = 6.8 Hz, C*H*$_3$, 6H), 1.11 – 1.01 (m, C*H*$_3$, 12H). ^{13}C NMR (126 MHz, CD_3CN) δ 144.81 (s), 132.24 (s), 130.99 (s), 130.38 (s), 129.79 (s), 129.14 (s), 123.78 (s), 77.26 (s), 27.52 (vt, $^{1}J_{PC}$ = 7.6 Hz), 21.71 (vt, $^{1}J_{PC}$ = 9.6 Hz), 19.69 – 19.18 (m), 19.05 (s), 16.82 (s). ^{31}P NMR (121 MHz, CD_3CN) δ 32.08 (s). ^{19}F NMR (282 MHz, CD_3CN) δ -79.33 (s). Anal. Calcd. for: $C_{30}H_{40}F_3NO_3P_2PdS$ (**2Pd-H**) (%): C, 50.04; H, 5.60; N, 1.95. Found: C, 50.25; H, 5.58; N, 1.81.

Synthesis of Complex 3Ni

Compound **2Ni** (53.8 mg, 0.103 mmol, 1 equiv.) was dissolved in benzene (*ca.* 5 mL) and transferred to a 20 mL scintillation vial equipped with a magnetic stirbar. Triethylammonium triflate (27.9 mg, 0.111 mmol, 1.08 equiv.) was added as a benzene solution (*ca.* 5 mL). The reaction mixture was allowed to stir for 3 hrs before volatiles were removed under reduced pressure. The material could be recrystallized from tetrahydrofuran:hexanes to yield the desired product as brown crystals sufficient for identification of the compound in the solid state. In acetonitrile the complex breaks up likely due to acetonitrile coordination. The sensitivity of the complex precluded further detailed characterization by NMR or elemental analysis. In d_8-tetrahydrofuran the ^{31}P NMR shows two very broad signals consistent with the solid state structure. By ^{1}H NMR very broad signals were observed precluding assignment and ^{13}C was too broad to observe assignable peaks. Yield: 36.8 mg (60 %). ^{31}P NMR (121 MHz, *d*$_8$-THF) δ 42.12 (broad s), 25.68 (broad s). ^{19}F NMR (282 MHz, *d*$_8$-THF) δ -78.96 (s).

Synthesis of Complex 4Ni(CO)

Compound **2Ni** (71.7 mg, 0.137 mmol, 1 equiv.) was dissolved in benzene (*ca.* 20 mL) and transferred to a Schlenk flask fitted with a screw-in Teflon stopper and equipped with a magnetic stirbar. This solution was degassed and CO (1.3 equiv.) admitted to the reaction flask. The solution stirred for 3 hrs during which time a lightening of the solution was observed. All volatiles were then removed under vacuum. The resulting brown residue was dissolved in benzene and transferred to a 20 mL scintillation vial. Lyophilization of the solvent yielded the desired clean product as a brown powder without further purification. Yield: 71.4 mg (94.5 %) ^{1}H NMR (500 MHz, C_6D_6) δ 8.58 (broad s, Py*H*, 2H), 7.34 – 7.26 (m, Ar*H*, 4H), 7.11 (t, $^{3}J_{HH}$ = 7.4 Hz, Ar*H*, 2H), 7.06 (t, $^{3}J_{HH}$ = 7.3 Hz, Ar*H*, 2H), 6.23 (s, Py*H*, 1H), 2.63 – 2.20 (m, C*H*,

2H), 2.19 – 1.94 (m, C*H*, 2H), 1.13 – 1.04 (m, C*H*$_3$, 6H), 1.00 (dd, $^3J_{PH}$ =14.6, $^3J_{HH}$ = 6.9 Hz, C*H*$_3$, 12H), 0.84 (dd, $^3J_{PH}$ = 6.8, $^3J_{HH}$ = 6.6 Hz, C*H*$_3$, 6H). ^{13}C NMR (126 MHz, C_6D_6) δ 197.31 (s), 148.37 (s), 145.30 (s), 134.32 (s), 130.54 (s), 129.60 (s), 129.06 (s), 128.20 (s), 83.07 (s), 28.52 (vt, $^1J_{PC}$ =10.6 Hz), 25.74 (vt, $^1J_{PC}$ = 6.5 Hz), 19.72 (t, $^2J_{PC}$ = 4.9 Hz), 18.81 (vt, $^2J_{PC}$ = 4.7 Hz), 18.14 (s), 17.70 (s). ^{31}P NMR (121 MHz, C_6D_6) δ 33.81 (s). IR(thin film, ATIR) ν_{CO}: 1930 cm^{-1}. Anal. Calcd. for: $C_{30}H_{39}NNiOP_2$ (**4Ni(CO)**) (%): C, 65.48; H, 7.14; N, 2.55. Found: C, 65.23; H, 6.87; N, 2.34.

Synthesis of Complex 4Ni(CO)-B(C_6F_5)$_3$

Compound **2Ni-B(C_6F_5)$_3$** (48.2 mg, 0.046 mmol, 1 equiv.) was dissolved in benzene (*ca.* 10 mL) and transferred to a Schlenk flask fitted with a screw-in Teflon stopper and equipped with a magnetic stirbar. This solution was degassed and CO (1.3 equiv.) admitted to the reaction flask. The solution stirred for 3 hrs during which time a lightening of the solution was observed. All volatiles were then removed under vacuum. The resulting brown residue was dissolved in benzene and transferred to a 20 mL scintillation vial. Lyophilization of the solvent yielded the desired clean product as a brown powder without further purification. Yield: 42.6 mg (86 %). ^{1}H NMR (300 MHz, C_6D_6) δ 8.03 (s, Py*H*, 2H), 7.59 (dd, $^3J_{HH}$ = 7.7, $^4J_{HH}$ = 2.9 Hz, Ar*H*, 2H), 7.04 (m, Ar*H*, 2H), 6.96 (d, $^3J_{HH}$ = 4.7 Hz, Ar*H*, 4H), 4.57 (t, $^2J_{PH}$ = 6.8 Hz, Py*H*, 1H), 2.17 (h, $^3J_{HH}$ = 7.0 Hz, C*H*, 2H), 1.74 (h, $^3J_{HH}$ = 6.9 Hz, C*H*, 2H), 0.87 – 0.73 (m, C*H*$_3$, 6H), 0.59 (m, C*H*$_3$, 18H). ^{13}C NMR (126 MHz, C_6D_6) δ 197.39 (s), 149.10 (s), 147.15 (s), 147.03 – 146.11 (m), 140.95 (s), 138.64 (s), 138.41 (s), 136.47 (m), 131.61 – 130.78 (m), 130.41 (d, $^2J_{PC}$ = 32.4 Hz), 129.19 (s), 128.66 (s), 128.18 (s), 119.03 (s), 113.82 (s), 68.61 (s), 27.30 (vt, $^1J_{PC}$ = 10.2 Hz), 24.29 (vt, $^1J_{PC}$ = 6.7 Hz), 19.07 – 18.32 (m), 17.92 – 16.97 (m), 16.69 (s). ^{31}P NMR (121 MHz, C_6D_6) δ 31.84 (s). ^{19}F NMR (282 MHz, C_6D_6) δ -130.79 (s), -

157.28 (s), -163.66 (s). IR(thin film, ATIR) ν_{CO}: 1976 cm^{-1}. Anal. Calcd. for: $C_{48}H_{39}BF_{15}NNiOP_2$ (**4Ni-B(C_6F_5)$_3$**) (%): C, 54.27; H, 3.70; N, 1.32. $C_{60}H_{51}BF_{15}NNiOP_2$ (**4Ni(CO)-B(C_6F_5)$_3$·2(C_6H_6)**) (%): C, 59.14; H, 4.22; N, 1.15. Found: C, 58.57; H, 4.32; N, 1.12.

Synthesis of Complex 4Ni(CO)-H

Compound **2Ni** (72.9 mg, 0.140 mmol, 1 equiv.) was dissolved in benzene (*ca.* 20 mL) and transferred to a Schlenk flask fitted with a screw-in Telfon stopper and equipped with a magnetic stirbar. This solution was degassed and CO (1.3 equiv.) admitted to the reaction flask. The solution stirred for 3 hrs during which time a lightening of the solution was observed consistent with the formation of **4Ni(CO)**. All volatiles were then removed under vacuum. The residue was then redissolved in tetrahydrofuran (*ca.* 4 mL) and transferred to a 20 mL scintillation vial equipped with a magnetic stirbar. Pyridinium triflate (31.98 mg, 0.140 mmol, 1 equiv.) was then added as a tetrahydrofuran solution (*ca.* 2 mL), which resulted in a color change from brown to a red brown. This reaction was allowed to stir for 1 hr before all volatiles were removed under reduced pressure to yield the desired product as a red brown powder. Yield: 52.0 mg (67.7 %). ^{1}H NMR (500 MHz, CD_3CN) δ 11.78 (broad s, N*H*, 1H), 7.84 (d, $^4J_{HH}$ = 3.7 Hz, Py*H*, 2H), 7.75 (m, Ar*H*, 2H), 7.63 (m, Ar*H*, 4H), 7.54 (m, Ar*H*, 2H), 4.79 (t, $^2J_{PH}$ = 6.1 Hz, Py*H*, 1H), 2.82 (h, $^3J_{HH}$ = 6.9 Hz, C*H*, 2H), 2.49 (h, $^3J_{HH}$ = 7.0 Hz, C*H*, 2H), 1.32 (dd, $^3J_{PH}$ = 12.2, $^3J_{HH}$ = 7.1 Hz, C*H*$_3$, 6H), 1.08 (m, C*H*$_3$, 12H), 0.88 (dd, $^3J_{PH}$ = 13.6, $^3J_{HH}$ = 7.0 Hz, C*H*$_3$, 6H). ^{13}C NMR (126 MHz, CD_3CN) δ 198.82 (s), 145.31 (vt, $^2J_{PC}$ = 11.5 Hz), 132.41 – 131.83 (m), 131.62 (d, $^1J_{PC}$ = 12.5 Hz), 130.50 (s), 129.66 (s), 129.10 (s), 113.51 (vt, $^3J_{PC}$ = 5.7 Hz), 66.74 (s), 27.55 (vt, $^1J_{PC}$ = 10.7 Hz), 24.75 (vt, $^2J_{PC}$ = 7.6 Hz), 19.22 (s), 18.19 (s), 17.54 (s), 17.01 (s). ^{31}P NMR (121 MHz, CD_3CN) δ 35.69 (s). ^{19}F NMR (282 MHz, CD_3CN)

δ -79.25 (s). IR(thin film, ATIR) ν_{CO}: 1975 cm^{-1}. Anal. Calcd. for: $C_{31}H_{40}F_3NNiO_4P_2S$ (**4Ni(CO)-H**) (%): C, 53.16; H, 5.76; N, 2.00. Found: C, 51.96; H, 5.39; N, 2.54.

Synthesis of Complex 4Ni(CO)-Me

Compound **2Ni-Me** (35.9 mg, 0.052 mmol, 1 equiv.) was dissolved in benzene (*ca.* 10 mL) and transferred to a Schlenk flask fitted with a screw-in Teflon stopper and equipped with a magnetic stirbar. This solution was degassed and CO (1.3 equiv.) admitted to the reaction flask. The solution stirred for 3 hrs during which time a lightening of the solution. All volatiles were then removed under vacuum. The resulting red brown residue was dissolved in acetonitrile and transferred to a 20 mL scintillation vial. Removal of the volatiles under reduced pressure yielded the desired clean product as a red brown powder without further purification. Yield: 34.7 mg (93 %). ^{1}H NMR (500 MHz, C_6D_6) δ 7.95 (dd, $^3J_{HH}$ = 7.8, $^4J_{HH}$ = 3.5 Hz, Ar*H*, 2H), 7.65 (d, $^4J_{HH}$ = 4.0 Hz, Py*H*, 2H), 7.37 (dd, $^3J_{HH}$ = 9.3, $^4J_{HH}$ = 5.7 Hz, Ar*H*, 2H), 7.22 (dd, J = 9.0, 5.8 Hz, Ar*H*, 2H), 7.16 (m, Ar*H*, 2H), 4.51 (t, $^2J_{PH}$ = 6.2 Hz, Py*H*, 1H), 3.75 (s, NC*H*$_3$, 3H), 2.34 – 2.22 (m, C*H*, 2H), 1.98 (p, $^3J_{HH}$ = 6.7 Hz, C*H*, 2H), 0.89 (m, C*H*$_3$, 12H), 0.70 (dd, $^3J_{PH}$ = 13.5, $^3J_{HH}$ = 6.8 Hz, C*H*$_3$, 12H). ^{13}C NMR (126 MHz, C_6D_6) δ 145.02 (vt, $^2J_{PC}$ = 11.4 Hz), 136.12 (s), 131.82 – 131.01 (m), 130.79 (s), 130.57 (s), 130.41 (s), 129.33 (s), 128.21 (s), 115.61 (s), 67.44 (s), 45.67 (s), 27.75 (vt, $^1J_{PC}$ = 10.4 Hz), 24.84 (vt, $^1J_{PC}$ = 7.1 Hz), 19.36 (s), 18.39 (s), 17.75 (s), 17.42 (s). ^{31}P NMR (121 MHz, C_6D_6) δ 34.74 (s). ^{19}F NMR (282 MHz, C_6D_6) δ -77.53 (s). IR(thin film, ATIR) ν_{CO}: 1966 cm^{-1}. Anal. Calcd. for: $C_{32}H_{42}F_3NNiO_4P_2S$ (**4Ni(CO)-Me**) (%): C, 53.80; H, 5.93; N, 1.96. Found: C, 54.09; H, 5.98; N, 1.71.

Synthesis of Complex 5Ni

Compound **2Ni** (98.8 mg, 0.189 mmol, 1 equiv.) was dissolved in tetrahydrofuran (*ca.* 5 mL) and transferred to a 20 mL scintillation vial equipped with a magnetic stirbar. While stirring vigorously, $[OMe_3][BF_4]$ (28.0 mg, 0.189 mmol, 1 equiv.) was added as a suspension in tetrahydrofuran (*ca.* 5 mL). The reaction mixture was allowed to stir for *ca.* 2 hrs during which time the $[Me_3O][BF_4]$ solubilized and a significant darkening of the solution to a color similar to **2Ni-Me** was observed. At this point, $[NO][BF_4]$ was added as a suspension in tetrahydrofuran (*ca.* 5 mL) and the vial was rapidly sealed. The reaction mixture was allowed to stir for 16 hrs during which time to solution a heterogenous brown with visible blueish precipitate forming upon standing. The reaction mixture was then filtered over a Celite pad and washed with copious tetrahydrofuran until washes became colorless leaving a blue colored precipitate. The product was eluted from the Celite pad using acetonitrile, and volatiles of the blue filtrate were removed under reduced pressure. The product could be purified by crystallization from acetonitrile:diethyl ether to yield the desired complex as blue crystals. Yield: 34 mg (24.3 %). The compound is unstable in solution and prone to decomposition. Peaks associated with the dominant decomposition product are indicated in the appropriate NMR spectra. ^{1}H NMR (500 MHz, CD_3CN) δ 9.01 (s, Py*H*, 2H), 8.16 – 8.05 (m, Ar*H*, 2H), 7.89 (m, Ar*H*, 4H), 7.81 – 7.74 (m, Ar*H*, 2H), 7.55 (s, Py*H*, 1H), 4.54 (s, NC*H*$_3$, 3H), 2.94 (m, C*H*, 4H), 1.19 – 1.04 (m, C*H*$_3$, 24H). ^{31}P NMR (121 MHz, CD_3CN) δ 31.31 (broad s). ^{13}C NMR (126 MHz, CD_3CN) δ 143.96 (s), 143.35 (s), 140.35 (d, $^{2}J_{PC}$ = 14.0 Hz), 134.41 (s), 133.27 (s), 132.20 (s), 132.09 (s), 131.46 (s), 131.07 (s), 128.50 (s), 128.04 (d, $^{1}J_{PC}$ = 24.4 Hz), 49.13 (s), 27.19 (s), 24.17 (s), 18.89 (s), 17.25 (s). IR(powder, ATIR) ν_{NO}: 1846 cm^{-1}. Anal. Calcd. for: $C_{30}H_{42}B_2F_8N_2NiOP_2$ (**5Ni**) (%): C, 48.63; H, 5.71; N, 3.78. $C_{30}H_{42}B_2F_8N_2NiOP_2$ (**5Ni-Me·MeCN**) (%): C, 49.15; H, 5.80; N, 5.37. Found: C, 48.13; H, 5.42; N, 5.15.

Synthesis of Complex 6Ni

Compound **2Ni** (24.6 mg, 0.047 mmol, 1 equiv.) was dissolved in benzene (*ca.* 2 mL) and transferred to a 20 mL scintillation vial equipped with a magnetic stirbar. Pinacol borane (6.9 μL, 0.047 mmol, 1 equiv.) was then added via Hamilton syringe. The reaction mixture was allowed to stir for 6 hrs before volatiles were removed under reduced pressure yielding the product without further purification. Yield: 29.1 mg (95 %). ^{1}H NMR (500 MHz, C_6D_6) δ 7.78 (dd, $^{3}J_{HH}$ = 7.4, $^{4}J_{HH}$ =2.9, Ar*H*, 1H), 7.55 (ddd, $^{3}J_{HH}$ = 7.3, $^{4}J_{HH}$ = 3.8, $^{4}J_{HH}$ = 2.2 Hz, Ar*H*, 1H), 7.33 (ddd, $^{3}J_{HH}$ = 8.8, $^{4}J_{HH}$ = 4.5, $^{4}J_{HH}$ = 2.2 Hz, Ar*H*, 1H), 7.13 – 7.10 (m, Ar*H*, 1H), 7.10 – 7.06 (m, Ar*H*, 2H), 7.05 – 7.00 (m, Ar*H*, 1H), 6.83 (d, $^{4}J_{HH}$ = 1.5 Hz, Py-(C3)*H*, 1H), 4.51 (dd, $^{1}J_{HH}$ = 13.6, $^{4}J_{HH}$ = 1.6 Hz, Py-(C4)*H*, 1H), 4.14 – 4.08 (m, Py-(C1)*H*, 1H), 3.78 (dtd, $^{1}J_{HH}$ = 13.6, $^{4}J_{PH}$ = 3.3, $^{3}J_{HH}$ = 1.2 Hz, Py-(C4)*H*, 1H), 2.35 – 2.21 (m, C*H*, 2H), 2.00 (pd, $^{3}J_{HH}$ = 7.0, $^{3}J_{HH}$ = 5.0 Hz, C*H*, 1H), 1.83 – 1.73 (m, C*H*, 1H), 1.25 – 1.15 (m, overlapping *i*Pr and pinacol CH_3, 9H), 1.12 (s, pinacol CH_3, 6H), 1.09 – 0.99 (m, *i*Pr CH_3, 12H), 0.98 (s, pinacol CH_3, 3H), 0.95 – 0.84 (m, *i*Pr CH_3, 6H). ^{13}C NMR (126 MHz, C_6D_6) δ 155.90 (d, $^{2}J_{PC}$ = 32.8 Hz), 150.24 (d, $^{2}J_{PC}$ = 15.2 Hz), 148.59 (d, $^{3}J_{PC}$ = 11.3 Hz), 148.33 (d, $^{2}J_{PC}$ = 11.5 Hz), 131.87 (d, $^{1}J_{PC}$ = 20.1 Hz), 131.01 (s), 129.66 (d, $^{1}J_{PC}$ = 8.4 Hz), 129.45 (s), 129.21 – 128.87 (m), 128.20 (s), 125.75 (m), 125.48 (s, Py(C2)), 120.81 (d, $^{4}J_{PC}$ = 5.3 Hz, Py(C3)), 82.33 (s), 71.21 (d, $^{2}J_{PC}$ = 14.6 Hz, Py(C5)), 59.22 (d, $^{2}J_{PC}$ = 10.9 Hz, Py(C1)), 52.41 (s, Py(C4)), 28.83 (d, $^{1}J_{PC}$ = 10.8 Hz), 27.73 (d, $^{1}J_{PC}$ = 15.1 Hz), 24.85 (s), 24.56 (s), 24.23 (d, $^{2}J_{PC}$ = 11.2 Hz), 23.83 (d, $^{2}J_{PC}$ = 15.7 Hz), 21.12 (d, $^{2}J_{PC}$ = 12.8 Hz), 20.91 (d, $^{2}J_{PC}$ = 7.9 Hz), 19.72 (d, $^{2}J_{PC}$ = 8.6 Hz), 19.38 (d, $^{2}J_{PC}$ = 11.3 Hz), 19.27 (d, $^{2}J_{PC}$ = 7.5 Hz), 18.97 (s), 18.88 (s), 18.78 (s). ^{31}P NMR (121 MHz, C_6D_6) δ 56.23 (d, J = 55.8 Hz), 44.70 (d, J = 55.6 Hz).

Synthesis of Complex 7Ni

Compound **2Ni** (213.4 mg, 0.408 mmol, 1 equiv.) was dissolved in benzene (*ca.* 10 mL) and transferred to a 20 mL scintillation vial equipped with a magnetic stirbar. Phenylsilane (50.4 μL, 0.408 mmol, 1 equiv.) was then added via Hamilton syringe. The reaction mixture was allowed to stir for 1 hr before volatiles were removed under reduced pressure yielding the product without further purification. Yield: 245 mg (95 %). ^{1}H NMR (500 MHz, C_6D_6) δ 7.70 (m, Ar*H*, 1H), 7.63 (m, Ar*H*, 1H), 7.50 (m, Ar*H*, 1H), 7.37 (t, $^{3}J_{HH}$ = 6.6 Hz, Ar*H*, 1H), 7.15 – 7.00 (m, Ar*H*, 6H), 6.40 (d, $^{4}J_{HH}$ = 7.9 Hz, Py-(C3)*H*, 1H), 5.29 (m, Si*H*$_2$, 2H), 4.18 – 4.09 (m, Py-(C1)*H*, 1H), 4.01 (d, $^{1}J_{HH}$ = 13.2 Hz, Py-(C4)*H*, 1H), 3.77 (dd, $^{1}J_{HH}$ = 13.1, $^{4}J_{HH}$ = 3.7 Hz, Py-(C4)*H*, 1H), 2.29 (m, C*H*, 2H), 2.05 (m, C*H*, 1H), 1.78 (m, C*H*, 1H), 1.24 (m, C*H*$_3$, 12H), 1.14 – 0.98 (m, C*H*$_3$, 6H), 0.94 (m, C*H*$_3$, 6H). ^{13}C NMR (126 MHz, C_6D_6) δ 155.77 (d, $^{2}J_{PC}$ = 33.4 Hz), 150.32 (d, $^{2}J_{PC}$ = 15.2 Hz), 148.80 (d, $^{1}J_{PC}$ = 10.9 Hz), 148.55 (d, $^{1}J_{PC}$ = 11.2 Hz), 135.69 (s), 134.91 (s), 133.13 (s), 131.72 (d, $^{3}J_{PC}$ = 7.2 Hz), 131.50 (d, $^{3}J_{PC}$ = 6.9 Hz), 131.16 (s), 130.11 (s), 129.76 (s), 129.59 (s), 129.43 (s), 128.90 (s), 128.30 – 127.87 (m), 125.83 (s), 125.58 (s), 124.96 (s, Py(C2)), 123.65 (d, J = 5.0 Hz, Py(C3)), 70.71 (d, $^{2}J_{PC}$ = 13.9 Hz, Py(C5)), 59.00 (d, $^{2}J_{PC}$ = 11.2 Hz, Py(C1)), 55.13 (s, Py(C4)), 28.71 (d), 27.68 (d, $^{1}J_{PC}$ = 15.3 Hz), 24.03 (d, $^{1}J_{PC}$ = 15.7 Hz), 21.44 (d, $^{1}J_{PC}$ = 12.7 Hz), 20.95 (m), 19.71 (d, $^{2}J_{PC}$ = 8.4 Hz), 19.45 (d, $^{2}J_{PC}$ = 10.9 Hz), 19.25 (d, $^{2}J_{PC}$ = 6.4 Hz), 19.10 (d, $^{2}J_{PC}$ = 4.5 Hz), 18.97 (d, $^{2}J_{PC}$ = 11.7 Hz), 18.86 (s). ^{31}P NMR (121 MHz, C_6D_6) δ 56.09 (d, *J* = 56.2 Hz), 44.77 (d, *J* = 56.1 Hz).

Synthesis of Complex 8Ni

Compound **2Ni-Me** (83.7 mg, 0.121 mmol, 1 equiv.) was dissolved in benzene (*ca.* 10 mL) and transferred to a 20 mL scintillation vial equipped with a magnetic stirbar. While stirring vigorously, sodium triethylborohydride (1 M toluene solution, 122 μL, 0.122 mmol, 1 equiv.)

was then added via Hamilton syringe resulting in an immediately lightening of the solution and precipitation of salts. The reaction was allowed to stir for 1 hr before the reaction mixture was filtered through a Celite pad. The volatiles of the filtrate were removed under reduced pressure yield the desired product without further purification. Yield: 62.4 mg (95 %). ^{1}H NMR (300 MHz, C_6D_6) δ 7.81 (dd, $^{3}J_{HH}$ = 7.7, $^{4}J_{HH}$ = 3.0, Ar*H*, 1H), 7.46 (dd, $^{3}J_{HH}$ = 7.7, $^{4}J_{HH}$ = 4.0, Ar*H*, 1H), 7.34 (dd, $^{3}J_{HH}$ = 7.4, $^{3}J_{HH}$ = 5.7, Ar*H*, 1H), 7.21 – 7.08 (m, Ar*H*, 1H), 7.10 – 7.03 (m, Ar*H*, 3H), 7.00 (m, Ar*H*, 1H), 5.85 (m, Py-(C3)*H*, 1H), 4.09 (t, $^{2}J_{PH}$ = 5.9 Hz, Py-(C1)*H*, 1H), 3.49 (d, $^{1}J_{HH}$ = 12.0 Hz, Py-(C4)*H*, 1H), 3.09 (d, $^{1}J_{HH}$ = 12.0 Hz, Py*H*, 1H), 2.36 (s, NC*H*$_3$, 3H), 2.34 – 2.17 (m, C*H*, 2H), 2.00 (m, C*H*, 1H), 1.81 (m, C*H*, 1H), 1.31 – 1.09 (m, C*H*$_3$, 12H), 1.03 – 0.84 (m, C*H*$_3$, 12H). ^{13}C NMR (126 MHz, C_6D_6) δ 156.12 (d, $^{2}J_{PC}$ = 33.1 Hz), 150.66 (d, $^{1}J_{PC}$ = 13.7 Hz), 148.75 (d, $^{1}J_{PC}$ = 11.9 Hz), 131.99 (d, $^{2}J_{PC}$ = 27.6), 131.17 (s), 130.10 (d, $^{4}J_{PC}$ = 5.5 Hz, Py(C3)), 129.58 (s), 129.33 (s), 129.29 – 129.16 (m), 125.82 (d, $^{3}J_{PC}$ = 4.3 Hz), 125.06 (d, $^{3}J_{PC}$ = 4.1 Hz), 120.05 (s, Py(C2)), 71.13 (d, $^{2}J_{PC}$ = 14.4 Hz, Py(C5)), 61.43 (d, $^{3}J_{PC}$ = 7.4 Hz, Py(C4)), 58.48 (d, $^{2}J_{PC}$ = 10.8 Hz, Py(C1)), 42.29 (s), 29.84 (s), 29.09 (d, $^{1}J_{PC}$ = 10.3 Hz), 27.63 (d, $^{1}J_{PC}$ = 15.2 Hz), 24.49 (d, $^{1}J_{PC}$ = 15.8 Hz), 21.51 (d, $^{1}J_{PC}$ = 12.9 Hz), 21.19 – 20.59 (m), 19.67 (m), 19.40 – 18.80 (m), 10.73 (s). ^{31}P NMR (121 MHz, C_6D_6) δ 56.52 (d, *J* = 56.5 Hz), 44.05 (d, *J* = 56.4 Hz). Anal. Calcd. for: $C_{30}H_{43}NNiP_2$ (**8Ni)** (%): C, 66.94; H, 8.05; N, 2.60. Found: C, 67.16; H, 7.96; N, 2.43.

Synthesis of Complex 2NiCl$_2$-B(C$_6$F$_5$)$_3$

1-B(C$_6$F$_5$)$_3$ (22.7 mg, 0.023 mmol, 1 equiv.) was dissolved in THF (*ca.* 2 mL) and transferred to a 20 mL scintillation vial equipped with a magnetic stirbar. $NiCl_2$(dme) (dme = dimethoxyethane) (5.1 mg, 0.023 mmol, 1 equiv.) was transferred as a suspension in miminal THF and the combined reaction mixture was allowed to stir overnight at room temperature.

Volatiles were then removed under reduced pressure and the residue dissolved in benzene and filtered through a Celite pad. The benzene filtrate was then lyophilized to afford the product as an orange-yellow powder. ^{1}H NMR (300 MHz, C_6D_6) δ 10.84 (s, 1H, Py-(C1)*H*), 8.57 (s, 2H, Py-(C3/C4)*H*), 7.41 (d, *J* = 7.6 Hz, 2H, Ar*H*), 7.03 – 6.94 (m, 4H, Ar*H*), 6.84 (t, *J* = 7.6 Hz, 2H, Ar*H*), 2.46 (s, 2H, C*H*), 1.63 – 1.52 (m, 2H, C*H*), 1.48 (m, 6H, CH_3), 1.10 (m, 6H, CH_3), 0.91 (m, 12H, CH_3). ^{31}P NMR (121 MHz, C_6D_6) δ 7.51. ^{19}F NMR (282 MHz, C_6D_6) δ -130.88, -155.80, -162.71.

Synthesis of Complex 2Ni-SiMe$_3$

2Ni (29.0 mg, 0.056 mmol, 1 equiv.) was dissolved in C_6D_6 and transferred to a J-young tube that had been previously silylated with trimethylsilyl chloride. Trimethylsilyl triflate (10.1 μL, 0.056 mmol, 1 equiv.) was added via Hamilton syringe and the tube was capped and inverted several times to ensure adequate mixing. The reaction mixture immediately turned from brown to a green/brown color during inversion. NMR data confirmed the quantitative conversion to **2Ni-SiMe$_3$** by ^{31}P NMR. The product is semistable in solution but will decompose to a mixture of species over time though this can be slowed in silylated glassware. ^{1}H NMR (300 MHz, C_6D_6) δ 7.26 – 7.00 (m, 10H, overlapping Ar*H* and Py-(C3/4)*H*), 2.70 (m, 2H, C*H*), 2.63 – 2.49 (m, 2H, C*H*), 1.99 (t, *J* = 5.4 Hz, 1H, Py-(C1)*H*), 1.26 – 1.18 (m, 6H, CH_3), 1.17 – 1.06 (m, 12H, CH_3), 1.00 (m, 6H, CH_3), 0.30 (s, 9H,SiCH_3). ^{31}P NMR (121 MHz, C_6D_6) δ 26.58. ^{19}F NMR (282 MHz, C_6D_6) δ -77.33.

Synthesis of Complex 4Ni(CN*t*Bu)

2Ni (14.9 mg, 0.029 mmol, 1 equiv.) was dissolved in C_6D_6 and transferred to a J-young tube. *Tert*-butyl isocyanide (3.23 μL, 0.029 mmol, 1 equiv.) was added via Hamilton syringe and the tube was capped and inverted several times to ensure adequate mixing. NMR data confirmed the formation of **4Ni(CN*t*Bu)** along with some small decomposition to free ligand (~17 %) by ^{31}P NMR. ^{1}H NMR (300 MHz, C_6D_6) δ 8.17 (s, 2H, Py-(C3/4)*H*), 7.47 (m, 2H, Ar*H*), 7.33 – 7.28 (m, 2H, Ar*H*), 5.51 (s, 1H, Py-(C1)*H*), 2.41 (m, 2H, C*H*), 2.11 (m, 2H, C*H*), 1.17 – 1.02 (m, 27H, overlapping CH_3 and C(CH_3)$_3$), 0.90 – 0.81 (m, 6H, CH_3). ^{31}P NMR (121 MHz, C_6D_6) δ 36.56. Crystals grown from this NMR reaction were used to obtain the solid-state structure for **4Ni(CN*t*Bu)**.

Synthesis of Complex 4Ni(CN*t*Bu)-Me

2Ni-Me (17.5 mg, 0.025 mmol, 1 equiv.) was dissolved in C_6D_6 and transferred to a NMR tube. *Tert*-butyl isocyanide (2.9 μL, 0.025 mmol, 1 equiv.) was then added by Hamilton syringe and the tube was capped and inverted several times to ensure adequate mixing. NMR data confirmed the quantitative formation of **4Ni(CN*t*Bu)-Me** by NMR. ^{1}H NMR (300 MHz, C_6D_6) δ 7.53 – 7.44 (m, 1H), 7.27 – 7.13 (m, 2H), 3.80 (t, J = 1.8 Hz, 1H), 3.62 – 3.54 (m, 0H), 2.35 (dq, J = 10.7, 3.5 Hz, 1H), 2.01 (dt, J = 13.4, 6.7 Hz, 1H), 1.18 (s, 3H), 1.00 – 0.91 (m, 1H), 0.91 – 0.83 (m, 1H), 0.82 – 0.69 (m, 2H). ^{31}P NMR (121 MHz, C_6D_6) δ 35.13. ^{19}F NMR (282 MHz, C_6D_6) δ -77.49.

Synthesis of Complex 4Ni(MeCN)-Me

2Ni-Me (20.0 mg, 0.029 mmol, 1 equiv.) was dissolved in MeCN. Volatiles were then removed under reduced pressure to afford **4Ni(MeCN)-Me** in quantitative yield. ^{1}H NMR (300 MHz, C_6D_6) δ 7.23 – 7.17 (m, 2H, Ar*H*), 7.16 – 7.07 (m, 6H, overlapping Ar*H* and Py-(C3/4)*H*), 7.02 – 6.98 (m, 2H, Ar*H*), 3.45 (s, 3H, NCH_3), 2.62 (t, *J* = 6.1 Hz, 1H, Py-(C1)*H*), 2.44 (m, 2H, C*H*), 2.20 – 2.05 (m, 2H, C*H*), 1.40 (s, 3H, CH_3CN), 1.00 – 0.90 (m, 12H, CH_3), 0.83 (m, 12H, CH_3). ^{31}P NMR (121 MHz, C_6D_6) δ 32.03. ^{19}F NMR (282 MHz, C_6D_6) δ -77.67.

Synthesis of Complex 4Ni(CN)-Me

2Ni-Me (15.3 mg, 0.022 mmol, 1 equiv.) was dissolved in THF (*ca.* 5 mL) and transferred to a 20 mL scintillation vial equipped with a magnetic stirbar. Tetrabutylammonium cyanide (6.0 mg, 0.022 mmol, 1 equiv.) was then added as a solution in *ca.* 1 mL THF and the reaction was allowed to stir for 3 hrs. Volatiles were then removed under reduced pressure. ^{31}P NMR data in C_6D_6 shows the clean conversion to a new species, however, removal of the tetrabutylammonium triflate with solvent washes of recrystallization proved difficult. Partial NMR data obtained for **4Ni(CN)-Me**. ^{1}H NMR (300 MHz, C_6D_6) δ 7.25 (d, *J* = 7.4 Hz, 2H, Ar*H*), 7.19 – 7.03 (m, 6H, Ar*H*), 6.55 – 6.49 (m, 2H, Py-(C3/4)*H*), 3.05 – 2.92 (m, 1H, Py-(C1)*H* overlapping with tetrabutylammonium triflate peaks), 2.64 (s, 3H, NCH_3), 2.56 (m, 4H, C*H*). ^{31}P NMR (121 MHz, C_6D_6) δ 36.02. ^{19}F NMR (282 MHz, C_6D_6) δ -77.67.

Synthesis of Complex 4Ni(N_3)-Me

2Ni-Me (22.0 mg, 0.032 mmol, 1 equiv.) was dissolved in THF (*ca.* 5 mL) and transferred to a 20 mL scintillation vial equipped with a magnetic stirbar. Tetrabutylammonium azide (9.1

mg, 0.032 mmol, 1 equiv.) was then added as a solution in *ca.* 1 mL THF and the reaction was allowed to stir for 3 hrs. Volatiles were then removed under reduced pressure. ^{31}P NMR data in C_6D_6 shows the clean conversion to a new species, however, removal of the tetrabutylammonium triflate with solvent washes of recrystallization proved difficult. Partial NMR data obtained for **4Ni(N$_3$)-Me**. ^{1}H NMR (300 MHz, C_6D_6) δ 7.26 (d, *J* = 7.5 Hz, 2H, Ar*H*), 7.13 (m, 6H, Ar*H*), 6.58 (s, 2H, Py-(C3/4)*H*), 2.71 (s, 3H, NC*H*$_3$), 2.67 – 2.56 (m, 2H, C*H*), 2.48 (s, 2H, C*H*), 2.25 (t, *J* = 6.2 Hz, 1H, Py-(C1)*H*). ^{31}P NMR (121 MHz, C_6D_6) δ 32.07. ^{19}F NMR (282 MHz, C_6D_6) δ -77.67.

Synthesis of 9Mo(CO)$_3$* from 1

1 (412.9 mg, 0.890 mmol, 1 equiv.) was dissolved in toluene (*ca.* 10 mL) and transferred to a Schlenk tube fitted with a screw-in Teflon stopper and a magnetic stirbar. $Mo(CO)_3(MeCN)_3$ (297 mg, 0.980 mmol, 1.1 equiv.) was then added as a suspension in *ca.* 10 mL of toluene and the reaction vessel was sealed and heated to 100 °C for 16 hrs. During this time the reaction mixture turned a red/orange color. Reaction volatiles were removed under reduced pressure. NMR in C_6D_6 revealed the predominant formation of **9Mo(CO)$_3$** along with an impurity (~20 %) with a very similar NMR characteristics (both ^{31}P and ^{1}H) believed to be a dimolybdenum complex where the pyridine nitrogen of one equivalent of **9Mo(CO)$_3$** is coordinated so a $Mo(CO)_n(L)_m$ species. Efforts to remove this impurity with solvent washes or recrystallizations proved unsuccessful so that material was carried forward as synthesized.

Synthesis of Complex 9Mo(CO)$_3$-H

9Mo(CO)$_3$* (55 mg) was dissolved in THF (*ca.* 5 mL) and transferred to a 20 mL scintillation vial equipped with a magnetic stirbar. Pyridinium triflate (18.9 mg, 0.082 mmol, 1 equiv. using effective mass if all **9Mo(CO)$_3$**) was then added as a solution in *ca.* 2 mL of THF and the reaction mixture was allowed to stir for 3 hrs at room temperature. Reaction volatiles were then removed under reduced pressure. The residue was then recrystallized from THF/pent vapor diffusion to yield clean **9Mo(CO)$_3$-H**. ^{1}H NMR (300 MHz, CD_3CN) δ 11.80 (broad s, 1H, Py-(N1)*H*), 7.96 (s, 2H, Py-(C3/4)*H*), 7.76 (m, 2H, Ar*H*), 7.60 – 7.54 (m, 2H, Ar*H*), 7.52 – 7.44 (m, 2H, Ar*H*), 7.24 (m, 2H, Ar*H*), 5.35 (s, 1H, Py-(C1)*H*), 3.28 (m, 2H, C*H*), 2.64 – 2.43 (m, 2H, C*H*), 1.59 – 1.40 (m, 6H, CH_3), 1.25 (m, 6H, CH_3), 1.15 (m, 12H, CH_3). ^{13}C NMR (126 MHz, CD_3CN) δ 217.62 (t, J_{CP} = 12.0 Hz), 211.49 (t, J_{CP} = 7.4 Hz), 207.86 (t, J_{CP} = 8.0 Hz), 145.19 (vt, J_{CP} = 10.4 Hz), 139.05 (s), 137.82 (vt, J_{CP} = 14.4 Hz), 130.79 (s), 130.14 (s), 129.91 (s), 128.95 (s), 119.46 (s), 69.68 (s), 34.23 (t, J_{CP} = 9.0 Hz), 27.29 (vt, J_{CP} = 11.3 Hz), 19.68 (s), 19.15 (s), 18.82 (s), 17.85 (s). ^{31}P NMR (121 MHz, CD_3CN) δ 54.63. ^{19}F NMR (282 MHz, CD_3CN) δ -79.35.

Synthesis of Complex 9Mo(CO)$_3$ from Complex 9Mo(CO)$_3$-H

9Mo(CO)$_3$-H (22.5 mg, 0.028 mmol, 1 equiv.) was dissolved in MeCN (*ca.* 5 mL) and transferred to a 20 mL scintillation vial equipped with a magnetic stirbar. Trimethylamine *n*-oxide (2.2 mg, 0.028 mmol, 1 equiv.) was then added as a solution in *ca.* 1 mL of MeCN) The reaction mixture was allowed to stir for 3 hrs at room temperature. Reaction volatiles were then removed under reduced pressure. Rather than decarbonylation, deprotonation and clean formation of **9Mo(CO)$_3$** without the impurity was obtained in quantitative yield. ^{1}H NMR (500 MHz, C_6D_6) δ 8.39 (s, 2H, Py-(C3/4)*H*), 7.16 (d, *J* = 7.8 Hz, 2H, Ar*H*), 7.00 (t, *J* = 7.5

Hz, 2H, Ar*H*), 6.90 (t, *J* = 7.5 Hz, 2H, Ar*H*), 6.77 (dd, *J* = 7.7, 1.9 Hz, 2H, Ar*H*), 6.15 (t, *J* = 2.0 Hz, 1H, Py-(C1)*H*), 2.67 (m, 2H, C*H*), 2.42 – 2.29 (m, 2H, C*H*), 1.52 (m, 6H, CH_3), 1.24 (m, 6H, CH_3), 1.00 (m, 12H, CH_3). ^{13}C NMR (126 MHz, C_6D_6) δ 222.27 (t, J_{CP} = 10.5 Hz), 212.98 (s), 211.76 (d, J_{CP} = 9.0 Hz), 148.33 (s), 146.51 (t, J_{CP} = 11.2 Hz), 139.91 (vt, J_{CP} = 11.5 Hz), 130.06(s), 129.31 (vt, J_{CP} = 4.1 Hz), 128.62 (s), 128.41 (s), 86.09 (s), 33.60 (vt, J_{CP} = 7.9 Hz), 28.22 (vt, J_{CP} = 10.5 Hz), 20.29 (s), 19.74 (vt, J_{CP} = 3.8 Hz), 19.27 (s), 18.48 (s). ^{31}P NMR (121 MHz, C_6D_6) δ 55.17. ^{19}F NMR (282 MHz, C_6D_6) δ -78.17.

Synthesis of Complex 9Mo(CO)$_3$-B(C$_6$F$_5$)$_3$

1-B(C$_6$F$_5$)$_3$ (56 mg, 0.057 mmol, 1 equiv.) was dissolved in toluene (*ca.* 5 mL) and transferred to a Schlenk tube fitted with a screw-in Teflon stopper and a magnetic stirbar. Mo(CO)3(MeCN)3 (17.4 mg, 0.057 mmol, 1 equiv.) was then added as a suspension in *ca.* 5 mL of toluene and then the reaction vessel was sealed and heated to 100 °C for 16 hrs. Reaction volatiles were then removed under reduced pressure to yield the desired product. ^{1}H NMR (300 MHz, C_6D_6) δ 8.11 (s, 2H, Py-(C3/4)*H*), 7.09 – 6.85 (m, 8H, Ar*H*), 4.99 – 4.95 (m, 1H, Py-(C1)*H*), 2.48 (m, 2H, C*H*), 2.10 – 1.97 (m, 2H, C*H*), 1.27 (dd, *J* = 15.4, 7.1 Hz, 6H, CH_3), 1.06 – 0.93 (m, 6H, CH_3), 0.88 – 0.77 (m, 12H, CH_3). ^{31}P NMR (121 MHz, C_6D_6) δ 55.97. ^{19}F NMR (282 MHz, C_6D_6) δ -130.44, -156.55 (t, *J* = 20.9 Hz), -163.32.

Crystallographic Information

CCDC 1400900-1400909 contain the supplementary crystallographic data for this paper. These data can be obtained free of charge from The Cambridge Crystallographic Data Centre via www.ccdc.cam.ac.uk/data_request/cif.

Refinement Details.

In each case, crystals were mounted on a glass fiber or nylon loop using Paratone oil, then placed on the diffractometer under a nitrogen stream. Low temperature (100 K) X-ray data were obtained on a Bruker APEXII CCD based diffractometer (Mo sealed X-ray tube, K_α = 0.71073 Å) or a Bruker PHOTON100 CMOS based diffractometer (Mo micro-focus sealed X-ray tube, K_α = 0.71073 Å). All diffractometer manipulations, including data collection, integration, and scaling were carried out using the Bruker APEXII software.[23] Absorption corrections were applied using SADABS.[24] Space groups were determined on the basis of systematic absences and intensity statistics and the structures were solved by direct methods using XS[25], by intrinsic phasing using XT (incorporated into SHELXTL), or by charge flipping using Olex2 and refined by full-matrix least squares on F^2.[26] All non-hydrogen atoms were refined using anisotropic displacement parameters. Hydrogen atoms were placed in the idealized positions and refined using a riding model. The structure was refined (weighed least squares refinement on F^2) to convergence. Graphical representation of structures with 50% probability thermal ellipsoids was generated using Diamond visualization software.[27] Data collection and refinement details are included in the Supporting Information.

Table 1. Crystal and refinement data for reported complexes.

Complex	**2Ni**	**2Pd**	**2Ni-B(C_6F_5)$_3$**	**2Pd-B(C_6F_5)$_3$**	**3Ni**
empirical formula	$C_{63}H_{90}N_2Ni_2P_4$	$C_{29}H_{39}NP_2Pd$	$C_{46}H_{43}B_5F_{15}NNiP_2$	$C_{47}H_{39}BF_{15}NP_2Pd$	$C_{65}H_{85}F_3N_2Ni_2O_3P_4S$
formula wt	1116.66	569.95	1069.51	1081.94	1272.71
T (K)	100	100(2)	99.99	100.03	100.01
a, Å	18.7148(7)	8.6112(7)	40.5679(17)	13.4502(7)	20.003(3)
b, Å	13.0646(5)	17.8635(16)	12.1876(4)	14.6571(7)	13.924(2)
c, Å	25.9359(9)	8.8154(11)	20.6773(7)	22.5392(11)	22.832(4)
α, deg	90	90	90	90	90
β, deg	109.324(2)	99.464(4)	114.405(2)	91.080(2)	22.832(4)
γ, deg	90	90	90	90	90
V, Å^3	5984.1(4)	1337.6(2)	9309.9(6)	4442.6(4)	6267.1(18)
Z	4	4	4	4	4
cryst syst	Monoclinic	Monoclinic	Monoclinic	Monoclinic	Monoclinic
space group	P 1 21/n 1	P 21	C 1 2/c 1	P 1 21/c 1	P 1 21/n 1
d_{calcd}, g/cm^3	1.239	1.415	1.526	1.618	1.349
θ range, deg	1.630-30.557	2.342 to 45.810	1.759 to 30.538	2.280 to 36.326	1.720-28.677
μ, mm^{-1}	1.058	0.831	0.582	0.589	0.792
abs cor	Semi-empirical from equivalents	Semi-empirical from equivalents	Semi-empirical from equivalents	Semi-empirical from equivalents	Semi-empirical from equivalents
GOF[c]	0.775	0.885	1.017	1.014	1.003
R1,[a] wR2[b] (I > 2σ(I))	0.0364, 0.0843	0.0639, 0.1107	0.0361, 0.0867	0.0414, 0.0897	0.0437, 0.0840

Table 2. Crystal and refinement data for reported complexes.

Complex	**2Ni-BCy$_2$OTf**	**2Pd-H**	**4Ni(CO)**	**4Ni(CO)-H**	**5Ni**
empirical formula	$C_{42}H_{61}BF_3NNiO_3P_2S$	$C_{30}H_{40}F_3NO_3P_2PdS$	$C_{30}H_{39}NNiOP_2$	$C_{31}H_{40}F_3NNiO_4P_2S$	$C_{64}H_{90}B_4F_{16}N_6Ni_2O_2P_4$
formula wt	848.43	720.03	550.27	700.35	1563.95
T (K)	100.01	100.01	100.0	99.98	100.11
a, Å	15.7224(11)	12.2515(8)	11.5436(5)	12.7394(14)	11.4094(4)
b, Å	12.6201(9)	11.1901(7)	15.7065(6)	15.2760(17)	11.4298(4)
c, Å	22.1023(15)	24.2291(15)	15.3374(5)	16.7217(19)	30.3230(12)
α, deg	90	90	90	90	92.4620(10)
β, deg	109.324(2)	102.437(3)	90.135(2)	101.186(2)	100.545(2)
γ, deg	90	90	90	90	107.826(2)
V, Å^3	4170.8(5)	3243.8(4)	2780.81(18)	3192.3(6)	3680.2(2)
Z	4	4	4	4	2
cryst syst	Monoclinic	Monoclinic	Monoclinic	Monoclinic	Triclinic
space group	P 1 21/c 1	P 1 21/c 1	P 1 21/c 1	P 1 21/c 1	P -1
d_{calcd}, g/cm^3	1.351	1.474	1.314	1.457	1.411
θ range, deg	2.522 to 30.530	1.702 to 30.570	1.764 to 30.552	1.822 to 30.519	2.981 to 78.736
μ, mm^{-1}	0.645	0.783	0.836	0.828	2.208
abs cor	Semi-empirical from equivalents	Semi-empirical from equivalents	Semi-empirical from equivalents	Semi-empirical from equivalents	Semi-empirical from equivalents
GOF[c]	1.041	1.076	1.005	1.050	1.078
R1,[a] wR2[b] (I > 2σ(I))	0.0417, 0.1143	0.0211, 0.0508	0.0321, 0.0724	0.0248, 0.0634	0.0810, 0.2035

Table 3. Crystal and refinement data for reported complexes.

Complex	**4Ni(CN*t*Bu)**	**9Mo(CO)$_3$-H**
empirical formula	$C_{34}H_{48}BF_3N_2NiP_2$	$C_{33}H_{40}F_3MoNO_6P_2S$
formula wt	605.39	793.60
T (K)	99.98	99.95
a, Å	17.460(2)	10.1276(2)
b, Å	10.8834(13)	24.7845(6)
c, Å	16.865(2)	14.5371(3)
α, deg	90	90
β, deg	94.574(7)	110.2770(10)
γ, deg	90	90
V, Å^3	3194.6(7)	3422.79(13)
Z	4	4
cryst syst	Monoclinic	Monoclinic
space group	P 1 2_1/c 1	P 1 2_1/c 1
d_{calcd}, g/cm^3	1.259	1.540
θ range, deg	1.170 to 36.520	2.296 to 30.525
μ, mm^{-1}	0.733	0.599
abs cor	Semi-empirical from equivalents	Semi-empirical from equivalents
GOF[c]	0.963	1.041
R1,[a] wR2[b] (I > 2σ(I))	0.0363, 0.1185	0.0211, 0.0493

[a] $R1 = \Sigma||F_o|-|F_c|| / \Sigma|F_o|$ [b] $wR2 = \{ \Sigma [w(F_o^2-F_c^2)^2] / \Sigma [w(F_o^2)^2] \}^{1/2}$ [c] $GOF = S = \{ \Sigma [w(F_o^2-F_c^2)^2] / (n-p) \}^{1/2}$

REFERENCES

1.(a) Allgeier, A. M.; Mirkin, C. A., *Angew Chem Int Edit* **1998,** *37*, 894-908; (b) Cisnetti, F.; Gibard, C.; Gautier, A., *J Organomet Chem* **2015,** *782*, 22-30.
2.(a) Cesar, V.; Castro, L. C. M.; Dombray, T.; Sortais, J. B.; Darcel, C.; Labat, S.; Miqueu, K.; Sotiropoulos, J. M.; Brousses, R.; Lugan, N.; Lavigne, G., *Organometallics* **2013,** *32*, 4643-4655; (b) Benhamou, L.; Cesar, V.; Gornitzka, H.; Lugan, N.; Lavigne, G., *Chem Commun* **2009**, 4720-4722; (c) Azoulay, J. D.; Rojas, R. S.; Serrano, A. V.; Ohtaki, H.; Galland, G. B.; Wu, G.; Bazan, G. C., *Angew Chem Int Edit* **2009,** *48*, 1089-1092; (d) Benhamou, L.; Vujkovic, N.; Cesar, V.; Gornitzka, H.; Lugan, N.; Lavigne, G., *Organometallics* **2010,** *29*, 2616-2630.
3.Bergbreiter, D. E.; Frels, J. D.; Rawson, J.; Li, J.; Reibenspies, J. H., *Inorganica Chimica Acta* **2006,** *359*, 1912-1922.
4.(a) Walter, M. D.; White, P. S.; Schauer, C. K.; Brookhart, M., *New Journal of Chemistry* **2011,** *35*, 2884-2893; (b) Mehendale, N. C.; Lutz, M.; Spek, A. L.; Klein Gebbink, R. J. M.; van Koten, G., *J Organomet Chem* **2008,** *693*, 2971-2981; (c) Rivada-Wheelaghan, O.; Dauth, A.; Leitus, G.; Diskin-Posner, Y.; Milstein, D., *Inorganic Chemistry* **2015,** *54*, 4526-4538; (d) Weisman, A.; Gozin, M.; Kraatz, H.-B.; Milstein, D., *Inorganic Chemistry* **1996,** *35*, 1792-1797; (e) Ashkenazi, N.; Vigalok, A.; Parthiban, S.; Ben-David, Y.; Shimon, L. J. W.; Martin, J. M. L.; Milstein, D., *Journal of the American Chemical Society* **2000,** *122*, 8797-8798; (f) Gauvin, R. M.; Rozenberg, H.; Shimon, L. J. W.; Ben-David, Y.; Milstein, D., *Chemistry – A European Journal* **2007,** *13*, 1382-1393.
5.(a) Herbert, D. E.; Lara, N. C.; Agapie, T., *Chem-Eur J* **2013,** *19*, 16453-16460; (b) Chao, S. T.; Lara, N. C.; Lin, S. B.; Day, M. W.; Agapie, T., *Angew. Chem. Int. Ed.* **2011,** *50*, 7529-7532; (c) Kelley, P.; Lin, S. B.; Edouard, G.; Day, M. W.; Agapie, T., *Journal of the American Chemical Society* **2012,** *134*, 5480-5483.
6.(a) Smith, R. C.; Protasiewicz, J. D., *Organometallics* **2004,** *23*, 4215-4222; (b) Morgan, B. P.; Smith, R. C., *J Organomet Chem* **2008,** *693*, 11-16; (c) Baratta, W.; Herdtweck, E.; Martinuzzi, P.; Rigo, P., *Organometallics* **2001,** *20*, 305-308; (d) Chen, C.-S.; Lin, C.-S.; Yeh, W.-Y., *J Organomet Chem* **2011,** *696*, 1474-1478; (e) Robertson, G. B.; Whimp, P. O., *Inorganic Chemistry* **1974,** *13*, 2082-2088; (f) Robertson, G. B.; Tucker, P. A.; Whimp, P. O., *Inorganic Chemistry* **1980,** *19*, 2307-2315; (g) Bennett, M. A.; Clark, P. W.; Robertson, G. B.; Whimp, P. O., *Journal of the Chemical Society, Chemical Communications* **1972**, 1011-1012; (h) Barrett, B. J.; Iluc, V. M., *Organometallics* **2014,** *33*, 2565-2574; (i) Barrett, B. J.; Iluc, V. M., *Inorganic Chemistry* **2014,** *53*, 7248-7259; (j) Okamoto, K.; Omoto, Y.; Sano, H.; Ohe, K., *Dalton Transactions* **2012,** *41*, 10926-10929; (k) Dixon, F. M.; Farrell, J. R.; Doan, P. E.; Williamson, A.; Weinberger, D. A.; Mirkin, C. A.; Stern, C.; Incarvito, C. D.; Liable-Sands, L. M.; Zakharov, L. N.; Rheingold, A. L., *Organometallics* **2002,** *21*, 3091-3093; (l) Dixon, F. M.; Masar, M. S.; Doan, P. E.; Farrell, J. R.; Arnold, F. P.; Mirkin, C. A.; Incarvito, C. D.; Zakharov, L. N.; Rheingold, A. L., *Inorganic Chemistry* **2003,** *42*, 3245-3255; (m) Xu, F.-B.; Li, Q.-S.; Wu, L.-Z.; Leng, X.-B.; Li, Z.-C.; Zeng, X.-S.; Chow, Y. L.; Zhang, Z.-Z., *Organometallics* **2003,** *22*, 633-640.
7.(a) Harrold, N. D.; Hillhouse, G. L., *Chemical Science* **2013,** *4*, 4011-4015; (b) Haas, T.; Kaspar, K.; Forner, K.; Drexler, M.; Fischer, H., *J Organomet Chem* **2011,** *696*, 946-955; (c) Laskowski, C. A.; Miller, A. J. M.; Hillhouse, G. L.; Cundari, T. R., *Journal of the American Chemical Society* **2011,** *133*, 771-773; (d) Iluc, V. M.; Miller, A. J. M.; Anderson, J. S.; Monreal, M. J.; Mehn, M. P.; Hillhouse, G. L., *Journal of the American Chemical Society* **2011,** *133*, 13055-13063; (e) Iluc, V. M.; Hillhouse, G. L., *Journal of the American Chemical Society* **2010,** *132*, 15148-15150; (f) Waterman, R.; Hillhouse, G. L., *Journal of the American Chemical Society* **2008,**

130, 12628-12629; (g) Kogut, E.; Wiencko, H. L.; Zhang, L.; Cordeau, D. E.; Warren, T. H., *Journal of the American Chemical Society* **2005,** *127*, 11248-11249; (h) Melenkivitz, R.; Mindiola, D. J.; Hillhouse, G. L., *Journal of the American Chemical Society* **2002,** *124*, 3846-3847; (i) Mindiola, D. J.; Hillhouse, G. L., *Journal of the American Chemical Society* **2002,** *124*, 9976-9977; (j) Mindiola, D. J.; Hillhouse, G. L., *Journal of the American Chemical Society* **2001,** *123*, 4623-4624.
8.Bull, J. A.; Mousseau, J. J.; Pelletier, G.; Charette, A. B., *Chem Rev* **2012,** *112*, 2642-2713.
9.(a) Takao, T.; Kawashima, T.; Kanda, H.; Okamura, R.; Suzuki, H., *Organometallics* **2012,** *31*, 4817-4831; (b) Kawashima, T.; Takao, T.; Suzuki, H., *Angew Chem Int Edit* **2006,** *45*, 7615-7618; (c) Harrison, D. P.; Welch, K. D.; Nichols-Nielander, A. C.; Sabat, M.; Myers, W. H.; Harman, W. D., *Journal of the American Chemical Society* **2008,** *130*, 16844-16845; (d) Mehnert, C. P.; Haggitt, J.; Green, M. L. H., *J Organomet Chem* **1998,** *550*, 63-70.
10.Suseno, S.; Agapie, T., *Organometallics* **2013,** *32*, 3161-3164.
11.Velian, A.; Lin, S. B.; Miller, A. J. M.; Day, M. W.; Agapie, T., *J Am Chem Soc* **2010,** *132*, 6296-6297.
12.Jiang, Y.; Blacque, O.; Fox, T.; Berke, H., *Journal of the American Chemical Society* **2013,** *135*, 7751-7760.
13.Welch, G. C.; Prieto, R.; Dureen, M. A.; Lough, A. J.; Labeodan, O. A.; Holtrichter-Rossmann, T.; Stephan, D. W., *Dalton Transactions* **2009**, 1559-1570.
14.CSD search run: 6-member ring with one N, any bonds between vicinal atoms, H or C substitution, Pd or Ni bound to any C atoms in the ring.
15.Iluc, V. M.; Miller, A. J. M.; Hillhouse, G. L., *Chem Commun* **2005**, 5091-5093.
16.(a) Haller, K. J.; Enemark, J. H., *Inorganic Chemistry* **1978,** *17*, 3552-3558; (b) Landry, V. K.; Parkin, G., *Polyhedron* **2007,** *26*, 4751-4757; (c) MacBeth, C. E.; Thomas, J. C.; Betley, T. A.; Peters, J. C., *Inorganic Chemistry* **2004,** *43*, 4645-4662; (d) Muñoz, S. B.; Foster, W. K.; Lin, H.-J.; Margarit, C. G.; Dickie, D. A.; Smith, J. M., *Inorganic Chemistry* **2012,** *51*, 12660-12668; (e) Wright, A. M.; Wu, G.; Hayton, T. W., *Journal of the American Chemical Society* **2012,** *134*, 9930-9933; (f) Puiu, S. C.; Warren, T. H., *Organometallics* **2003,** *22*, 3974-3976; (g) Varonka, M. S.; Warren, T. H., *Organometallics* **2010,** *29*, 717-720.
17.McSkimming, A.; Colbran, S. B., *Chem Soc Rev* **2013,** *42*, 5439-5488.
18.(a) Gunanathan, C.; Milstein, D., *Accounts of Chemical Research* **2011,** *44*, 588-602; (b) Kundu, S.; Brennessel, W. W.; Jones, W. D., *Inorganic Chemistry* **2011,** *50*, 9443-9453; (c) Gunanathan, C.; Shimon, L. J. W.; Milstein, D., *Journal of the American Chemical Society* **2009,** *131*, 3146-3147; (d) Gunanathan, C.; Milstein, D., *Angewandte Chemie International Edition* **2008,** *47*, 8661-8664; (e) Gunanathan, C.; Gnanaprakasam, B.; Iron, M. A.; Shimon, L. J. W.; Milstein, D., *Journal of the American Chemical Society* **2010,** *132*, 14763-14765; (f) Ohtsu, H.; Tanaka, K., *Angewandte Chemie International Edition* **2012,** *51*, 9792-9795; (g) Koizumi, T.-a.; Tanaka, K., *Angewandte Chemie International Edition* **2005,** *44*, 5891-5894; (h) McSkimming, A.; Bhadbhade, M. M.; Colbran, S. B., *Angew Chem Int Edit* **2013,** *52*, 3411-3416.
19.Henthorn, J. T.; Lin, S.; Agapie, T., *Journal of the American Chemical Society* **2015,** *137*, 1458-1464.
20.(a) Buss, J. A.; Agapie, T., *Nature* **2016,** *529*, 72-75; (b) Buss, J. A.; Edouard, G. A.; Cheng, C.; Shi, J.; Agapie, T., *Journal of the American Chemical Society* **2014,** *136*, 11272-11275.
21.Pangborn, A. B.; Giardello, M. A.; Grubbs, R. H.; Rosen, R. K.; Timmers, F. J., *Organometallics* **1996,** *15*, 1518-1520.
22.Fulmer, G. R.; Miller, A. J. M.; Sherden, N. H.; Gottlieb, H. E.; Nudelman, A.; Stoltz, B. M.; Bercaw, J. E.; Goldberg, K. I., *Organometallics* **2010,** *29*, 2176-2179.

23.APEX2, Version 2 User Manual, M86-E01078, Bruker Analytical X-ray Systems, Madison, WI, June 2006.
24.Sheldrick, G.M. "SADABS (version 2008/1): Program for Absorption Correction for Data from Area Detector Frames", University of Göttingen, 2008.
25.Sheldrick, G.M. (2008). Acta Cryst. A64, 112-122.
26.Dolomanov, O.V. (2009). OLEX2. J. Appl. Cryst. 42, 339-341.
27.Brandenburg, K. (1999). DIAMOND. Crystal Impact GbR, Bonn, Germany.